Understanding Physical Mechanisms Governing the Response of Perovskite Solar Cells During Efficiency Measurement

Master Thesis presented in the course “Renewable Energy Systems – Environmental and Process Engineering” at HAW Hamburg

Supervised by:
Prof. Dr. Fritz Dildey
Dr. Ricky Dunbar

Author:
Moustafa, Walied
Matrikelnummer: **2000938**

Newcastle,
01.04.2016

Hochschule für Angewandte Wissenschaften Hamburg
Hamburg University of Applied Sciences

ABSTRACT

This study investigates the influence of different physical mechanisms on the electrical behaviour of Perovskite photovoltaic cells. An investigation of the problem of ambiguous results during electrical property measurement and the lack of the comparability of these results is conducted. It aims at contributing to the establishment of a guideline for these measurements by proposing a procedure to improve I-V curve measurement. Three different $CH_3NH_3PbI_3$ inverted structure cells were mainly studied, one fabricated by the author, the other two fabricated by a research group from the University of Oxford. The influence of irradiance level, temperature, voltage steps of different sizes, influence of time as well as light soaking treatment is studied. A procedure of estimating appropriate dwell times for the I-V curve measurement is proposed and tested on a silicon, dye and Perovskite cell. According to that procedure the cell's electrical parameters are measured in a steady state, thus improving the comparability of different cells as they are all measured the same state. A memory effect (lasting more than six hours) is identified as a reason for the poor reproducibility of transient current behaviour and intensely investigated. The cell's electrical behaviour does change depending on the history of exhibition to light and testing conditions but does return to an initial state after a sufficient resting time in the dark. That effect is found to be existing for the Oxford as well as the author's cell yet expressed in different ways. Whereas the author's cell's transient current behaviour is impaired by that memory effect, the effect is expressed in the Oxford cell as a memory of light soaking history. An improvement of the cells open circuit voltage and maximum power due to a light soak is observed. Once light soaked once that is state re-achieved quickly even after longer periods in the dark of more than 12 hours. Giving the cells a sufficient resting time in the dark (two days), the memory effect is fully cleared. The attempt is made to clear the cell's memory in few minutes to shorten measurement procedures in general. A partial recovery of the cell's initial state is reproducibly achieved. Further approaches for future research are proposed including the proposals for the memory clearance well and a way of utilizing the dwell time estimation method.

CONTRIBUTIONS TO CONFERENCE PRESENTATIONS

Aside from the Master Thesis, one conference paper one oral presentation can be listed as an outcome of the Master Project.

Oral presentation:

Ricky B. Dunbar, Walied Moustafa, Ben Duck, Kenrick F. Anderson, Timothy W. Jones, Christopher J. Fell, Gregory J. Wilson, "Pre-conditioning routines for efficiency measurements of perovskite solar cells", *International Conference on Hybrid and Organic Photovoltaics (HOPV16)*, Swansea (UK), July 2016

Paper:

Ricky B. Dunbar, Walied Moustafa, Noel Duffy, Ben Duck, Kenrick F. Anderson, Timothy W. Jones, Christopher J. Fell, Gregory Wilson, "An investigation of pre-conditioning for efficiency measurements of perovskite solar cells ", *32nd European Photovoltaic Solar Energy Conference and Exhibition (EU PVSEC)*, Munich, June 2016

TABLE OF CONTENTS

1 Introduction 1

2 The Perovskite Photovoltaic Cell 2

3 Fabrication and Measurement Methods 7

3.1 Cell fabrication 9

3.2 Measurement of electrical properties 12

3.3 Activation energy 16

4 Experiments and Results 18

4.1 Cell fabrication 18

4.2 The three cells 18

4.3 Measurement and calculation of τ for the dwell time estimation 22

4.4 Temperature and light level influence 26

4.5 Activation energies 30

4.6 Light soak influence 34

4.7 Memory effect in the W cell and current retardation 38

5 Conclusion 49

6 Outlook 51

7 References 52

8 Supplementary Information 54

1 INTRODUCTION

With the rise of attention on photovoltaic cells based on Perovskite materials in the scientific community, it is imperative to have a reliable and reproducible way of measuring cell parameters. The devices should be comparable to other cells with different architectures or materials, not only Perovskite but also silicon or organic cells. On the one hand a comparable characterization of Perovskite cells is of highest interest for scientific research. On the other hand it is absolutely necessary for the commercialization of Perovskite cells.

Yet the determination of e.g. the cell efficiency or I-V curves remains imprecise due to hysteresis effects and high output current stabilization times of hundreds of seconds depending on the preconditioning of the cell.[1] The mechanisms causing the measurement difficulties are not understood yet and currently subject to investigation.[2] Mechanisms in question would be ion migration, trapping/de-trapping, ferroelectric behaviour. [3]

Currently the measurement of I-V curves is defined in IEC60904-3. However whilst measuring current-voltage behaviour according to this standard varying results can be determined.

The measurement is carried out via a voltage sweep through the cell voltage range of interest while applying standard testing conditions. Ideally the measurement is performed after the current reaches a steady state. While silicon cells react sufficiently fast to changes of the applied voltage Perovskite cells respond much slower resulting in different behaviour depending on the voltage sweep rate and direction.[2] It has been shown that different dwell times, the waiting time after each voltage change until the measurement is performed, lead to different measurement results.[4]

This study attempts to understand how physical parameters (such as irradiance level, temperature and time) influence the electrical behaviour of the cells and what can be done to diminish current retarding effects to obtain reproducible results for the measurement of the electrical behaviour. Therefore a method is proposed to estimate suitable dwell times.

Ultimately a procedure to precisely and reproducibly determine the electrical properties of Perovskite cells is to be found. The aim of this work is to lay a foundation, based on understanding Perovskite cell's transient and non-time resolved electrical behaviour, to elaborate a measurement procedure meeting the mentioned requirements.

2 THE PEROVSKITE PHOTOVOLTAIC CELL

Perovskite cells have convincing features. A few examples are given in the following.

They show a strong light absorptance (due to direct bandgap properties similar to GaAs as it can be seen in Figure 1) [5], with an absorption coefficient of $CH_3NH_3PbI_3$ around $10^5\,cm^{-1}$ [6] and a direct band gap of ≈1.6 eV [7].

They can be fabricated at low temperatures (140 °C as shown for a planar structure by Qing et al. [8]) since CH_3NH_3I and PbI_2 crystallize at temperatures of 70 to 100 °C forming $CH_3NH_3PbI_3$ [9].

Low charge carrier recombination rates are observed (with values of $15 \times 10^6 \frac{1}{s}$ monomolecular rate constant, $0.6 \times 10^{-10} \frac{cm^3}{s}$ bimolecular rate constant and $1.6 \times 10^{-28} \frac{cm^6}{s}$ Auger rate constant [10]), a dielectric constant ε_0=1000 in the dark, that is further increasing under illumination[11], long carrier diffusion lengths (100 nm and more [12]) and low exciton binding energies (37-50 meV [13]). Unfortunately some negative attributes have to be mentioned as well e.g. the usage of lead for several state of the art architectures and a very fast degradation of the Perovskite, if exposed to humidity.[5]

A solution to the degradation problem is subject to research and the encapsulation of the cells seems to be a suitable solution, improving the long term stability of the cells.[14]

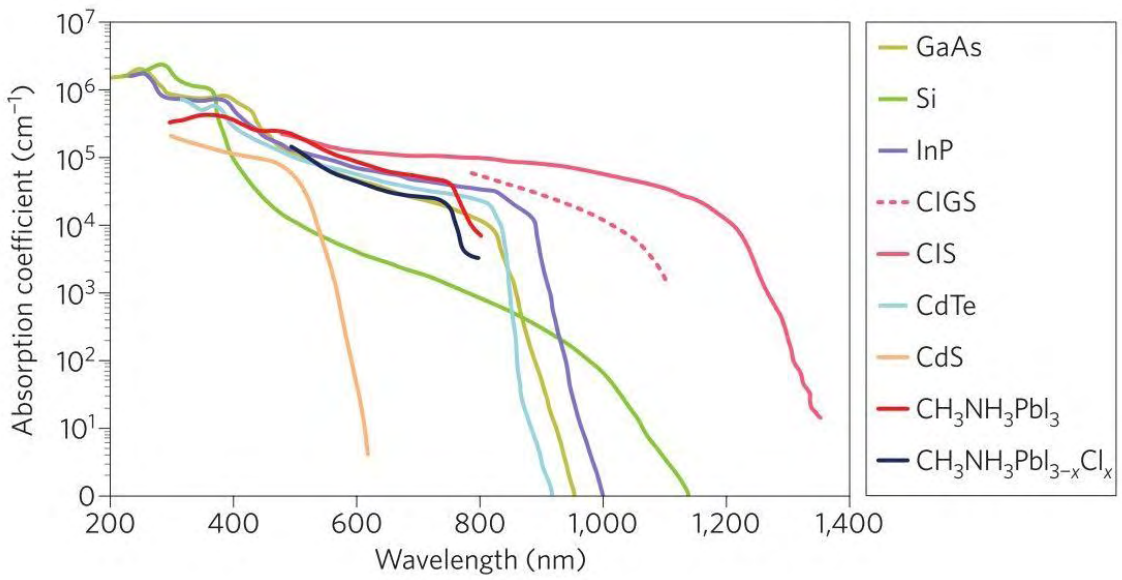

Figure 1: Absorption coefficients. Figure taken from Green, Ho-Baillie and Snaith [5]

Structure

The structure of the Perovskite materials can be described with the general formula ABX_3. A and B are both different cations, with A (organic cation, usually methylammonium with CH_3NH_3 and "MA" as abbreviation) being of larger size than B (metal cation, usually lead, Pb). X is a halide anion (I^-, Cl^- or Br^-).[15] The three dimensional arrangement of the crystal can be seen in Figure 2. The metal cation and the halide anion are forming an octahedron with the metal cation in the middle. Several conjoined octahedra are then forming the lattice with the organic anion filling the void.[6]

Through the dispersion interaction between methyl and iodide ions, the organic component influences the inorganic framework.[6] But this bonding is weak and can be easily distorted by temperature effects.[6]

In the case of CH3NH3PbI3 three crystal systems can be observed.[6] Orthorhombic phase for up to 161.4 K, Tetragonal phase from 161.4 K to 330.4 K, and cubic phase for temperatures above 330.4 K.[6]

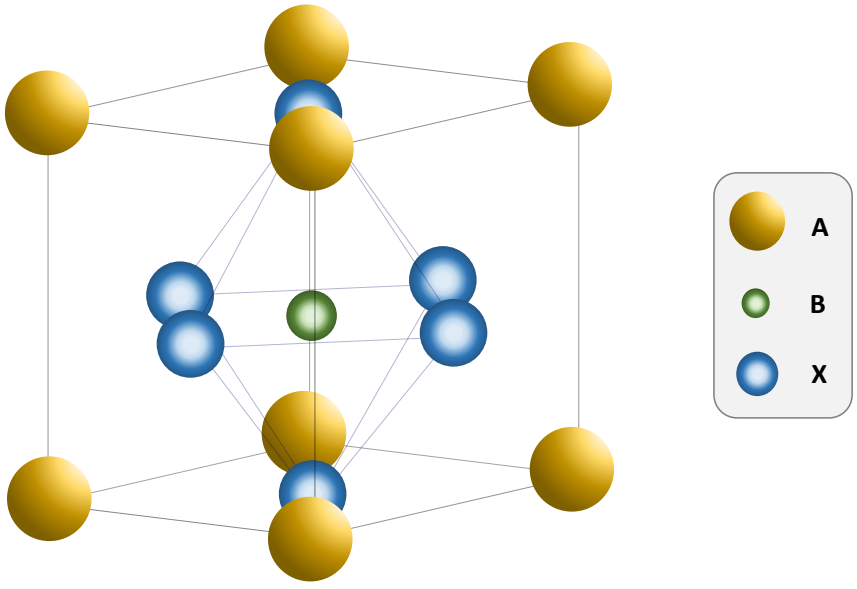

Figure 2: General Perovskite crystal structure

Currently the most promising materials for high efficient Perovskite photovoltaic cells are methylammonium lead triiodide ($CH_3NH_3PbI_3$) and its iodide chloride equivalent ($CH_3NH_3PbI_{3-x}Cl_x$).[15] A merit of the material is its ambipolar charge transport.[15] Most semiconductors have unequal balanced electron and hole masses. This Perovskite material is different as it has a fairly good balance between electron and hole masses (*electron effective mass = 0.23* m_0 ; *hole effective mass = 0.29* m_0).[15] According to Hsiao et al. Bulk polarisation during charge transport and

collection can be influenced by ambipolar charge transport (with the influence neither being quantified nor qualified by Hsiao himself, it can be argued from the information given, that bulk polarisation would occur less distinct as both, holes and electrons would be able to balance out and therefore positively influencing the parameters named in the following), hence leading to a change in short circuit current, open circuit voltage and the fill factor of PV cells.[15] Due to the ambipolar properties Perovskite can show both n- and p-type-material behaviour.[15]

The organic material ($CH_3NH_3^+$) is not expected to have a direct influence on transport or optical properties.[6] Yet a change of crystal properties due to the temperature effects affecting the organic material will indirectly influence the transport and optical properties.[6] With the bond length between Pb and I decreasing for the different phases from tetragonal (3.22 Å) to orthorhombic (3.18 Å) to pseudo-cubic (3.14 Å) the band widths increase due to an increased interaction between Pb and I. The wider band width leads to smaller band gaps (0.67 eV for pseudo cubic and 1.27 eV for tetragonal). Therefore the tetragonal phase at medium temperatures has an ideal bandgap as a photon absorber.[6] The highest charge carrier mobility is found for the pseudo cubic phase at high temperatures with values of $31.5 \times 10^3 \frac{\mathrm{cm}^2}{\mathrm{Vs}}$ (compared to 23.4 and $21.6 \times 10^3 \frac{\mathrm{cm}^2}{\mathrm{Vs}}$ for the tetragonal and the orthorhombic phase).[6] Hence for a maximal performance a balance should be found between both effects.[6]

Carrier diffusion length and exciton binding energy

With carrier diffusion length of ≈100 nm and ≈1 µm in solution processed polycrystalline $CH_3NH_3PbI_3$ and $CH_3NH_3PbI_{3-x}Cl_x$ Perovskite material can easily compete with organic materials (typical diffusion length of ≈10 nm [15]) [16] but is not as good as polycrystalline silicon (20-80 µm [17]).

Reaching a low value of about 37 meV[18] as exciton binding energy, $CH_3NH_3PbI_3$ performs better than organic materials (1.2 eV [19]). A modification of the binding energy is possible via application of interfacial layers, doping core-shell metal nano particles into Perovskites and different halogen elements.[15][20] Both properties, the high diffusion length together with the low exciton binding energy are important for high power conversion efficiencies of photovoltaic cells.[15]

Morphology and defects

Whereas polycrystalline Perovskites show defects, single crystals have low trap state densities in the order of 10^{10} cm^{-3}.[21] Grainsize and shape of the material can enormously influence the performance of the cell.[15] By adjusting the conditions under which the Perovskite is being

processed the morphology of the material can be easily changed.[22] This leaves plenty of room for research and engineering.

Absorption range

The absorption of spectrum of $CH_3NH_3PbI_3$ spans over a broad range from ultraviolet up to near infrared.[23] The external quantum efficiency and the integrated current density can be seen in Figure 3.

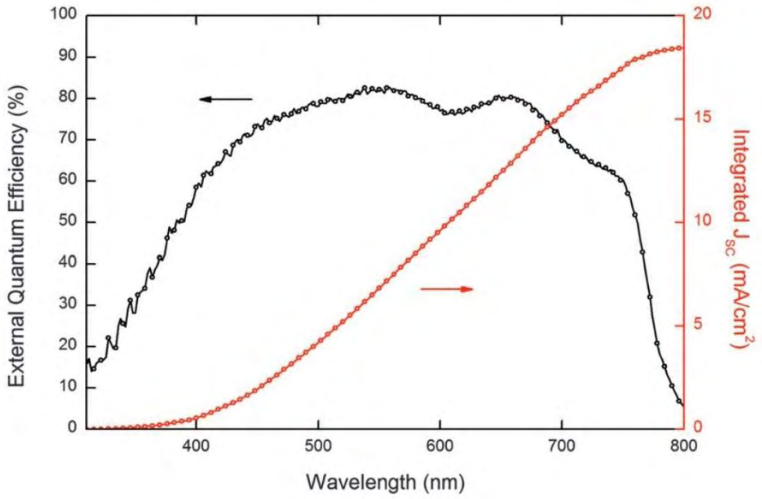

Figure 3: External quantum efficiency for MAPbI3-based cell at room temperature. Figure taken from Quarti et al.[23]

Ferroelectric behaviour

Perovskites show ferroelectric behaviour, their electric polarization can be reversed by the application of an external field. The ferroelectric field separates exciton and acts similar to a p-n-junction.[24] Tuning of these properties can be achieved by manipulation of organic cations and change of metal atoms in the crystal. Introduction of cations with different dipole strengths naturally affects the dielectric properties.[15]

The application of an external electrical field changes the orientation of the MA ions, which are highly rotatable, forming ordered domains with local potential fields.[25]

The ferroelectric polarization influences carrier collection, recombination and charge transport in a PV cell and might have a positive impact on charge separation and carrier lifetime.[15] That influence of polarized regions is strong enough to be described by Frost et al. as ferroelectric highways. There charge carriers can diffuse towards the electrodes without being influenced by

the opposing charge. These highways are suspected to be the origin of the long carrier diffusion lengths.[24]

Ions

Since Perovskite has the general formula A B X_3, the charge of one A and B cation have to match the charge of three X anions. Looking at halide Perovskite the halide X part has a single negative charge which is to be matched with three positive charges distributed over A and B [24] leaving us two possibilities:

1. $A^+ \quad B^{2+} \; X_3^-$
2. $A^{2+} \; B^+ \quad X_3^-$

Perovskite with the formula $CH_3NH_3PbI_3$ is composed of Pb^{2+}, $CH_3NH_3^+$ and I^-. These ions ability of vacancy assisted migration is suspected to influence charge carrier mechanics to an extend that hybrid halide Perovskite may be considered as ionic-electronic conductor.[26]

Vacancy mediated diffusion due to defects or non-stoichiometry is a common reason for ionic movement (hopping between neighbouring positions).[26] With an estimated diffusion coefficient of 10^{-12} cm^2s^{-1} and a theoretically calculated activation energy of 0.58 eV for I^- compared to 10^{-16} cm^2s^{-1} and 0.84 eV for $CH_3NH_3^+$, I^- can most likely be considered as the majority ionic carrier (Pb^{2+} has a theoretically calculated activation energy of 2.31 eV) as Pb^{2+} and $CH_3NH_3^+$ are less likely to overcome their activation energy level at room temperature.[26]

Meloni et al. report averaged activation energies for $MAPbI_3$ cells of 0.314 eV for 1 sun and 0.341 eV for 0.1 - 0.2 suns.[27] For $MAPbBr_3$, an averaged activation energy of 0.168 eV at 1 sun was found.[27]

3 FABRICATION AND MEASUREMENT METHODS

Troublesome measurements of I-V curves due hysteresis effects and different measurement results for different dwell [4] and light soaking times cause unpredictably long measurement durations. Since short measurement durations are desirable in general and extensive measurements might damage the cells in particular, a method to swiftly estimate necessary voltage dwell times rather than trial and error should be developed. The impact of dwell times on the measurement of different cell parameters has already been studied[4] and can be seen in Figure 4. Longer dwell times lead to more stable signals and more reliable results.

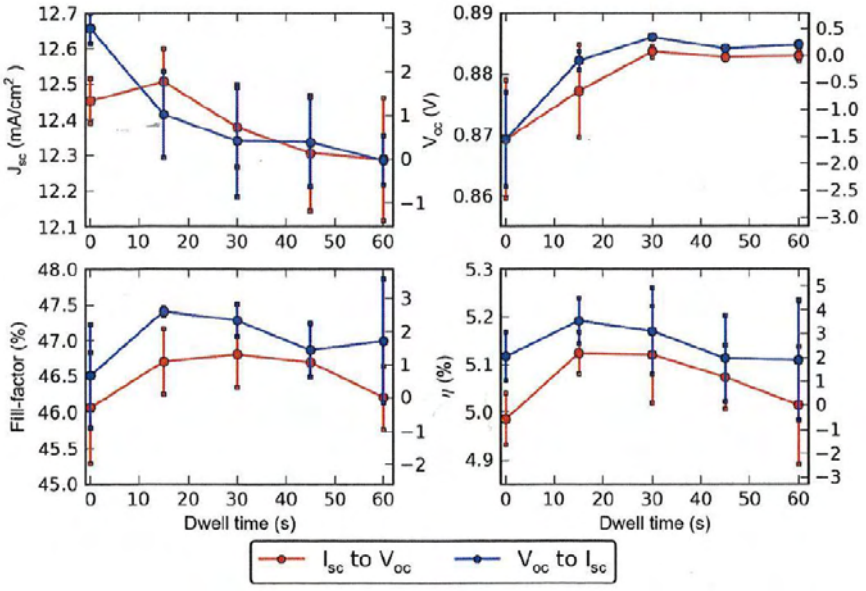

Figure 4: Impact of dwell times on different cell parameters, figure taken from Dunbar et al.[4]

Measurement of an I-V curve is basically a current measurement at certain cell voltages of the curve. The resolution of the measurement depends on the voltage step size. The term dwell time describes the period of time between a change of the cell voltage and the measurement of the current given the cell to stabilize the output signal. If the result of the I-V curve measurement differs depending on the dwell time at each voltage step, then a transient process can most likely be observed after each cell voltage change.

In the case of a stabilisation of the current after a change of the voltage, a time constant τ can be obtained. This τ value should bear information about the necessary dwell times. 99.3% of the currents maximum value would be reached after a dwell time of 5 τ as it can be seen in Figure 5.

An estimation of appropriate dwell times using these τ values should result in a reproducible and comparable measurement of the highest possible efficiency of the cell.

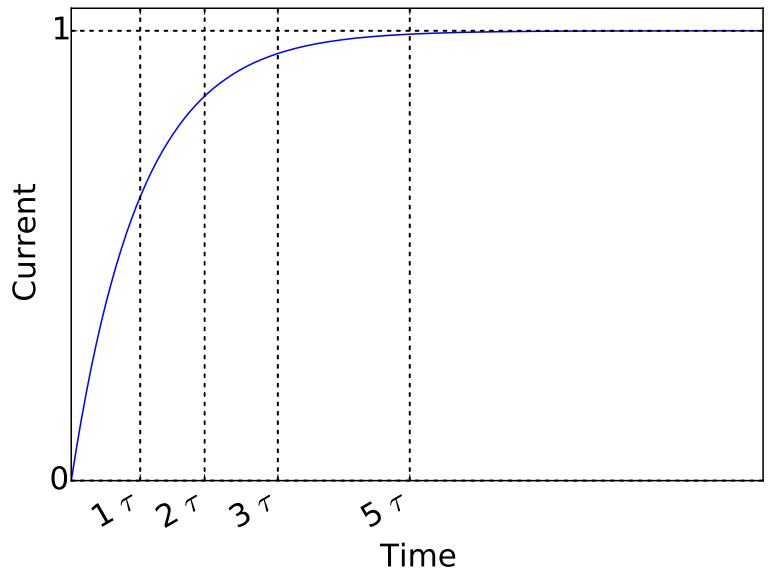

Figure 5: Expected transient current behaviour after a change in the cell voltage

Naturally the τ value will differ for different cell voltages due to changes in the internal fields in the cell. Therefore the highest τ value is predicted to be a suitable guess for the dwell time in the I-V measurement.

Hence the proposed method to obtain comparable cell performance results and resolve the dwell time uncertainty problem is to gather τ the values and use 5 times the highest τ value as a dwell time for the I-V scan.

3.1 CELL FABRICATION

The cells fabricated for this project had an inverted Perovskite structure as it can be seen in Figure 6 and were made of ITO|PEDOT:PSS|Perovskite|PCBM|Ag. PEDOT, poly(3,4-ethylenedioxythiophene), doped with PSS, poly(styrene sulfonic acid), is a transparent, highly conductive ($\approx 10 \frac{S}{cm}$) material [28] that can be used as a hole transport material [29]. PCBM (methanofullerene [6,6]-phenyl C_{61}-butyric acid methyl ester) is commonly used as an electron transport material.[30]

PEDOT:PSS, Perovskite and PCBM were deposited via spin coating with typical thicknesses of 55 nm, 210 nm and 110 nm, respectively. Silver has been evaporated on top of the cell. The glass substrates covered with ITO are a premanufactured, purchased product.

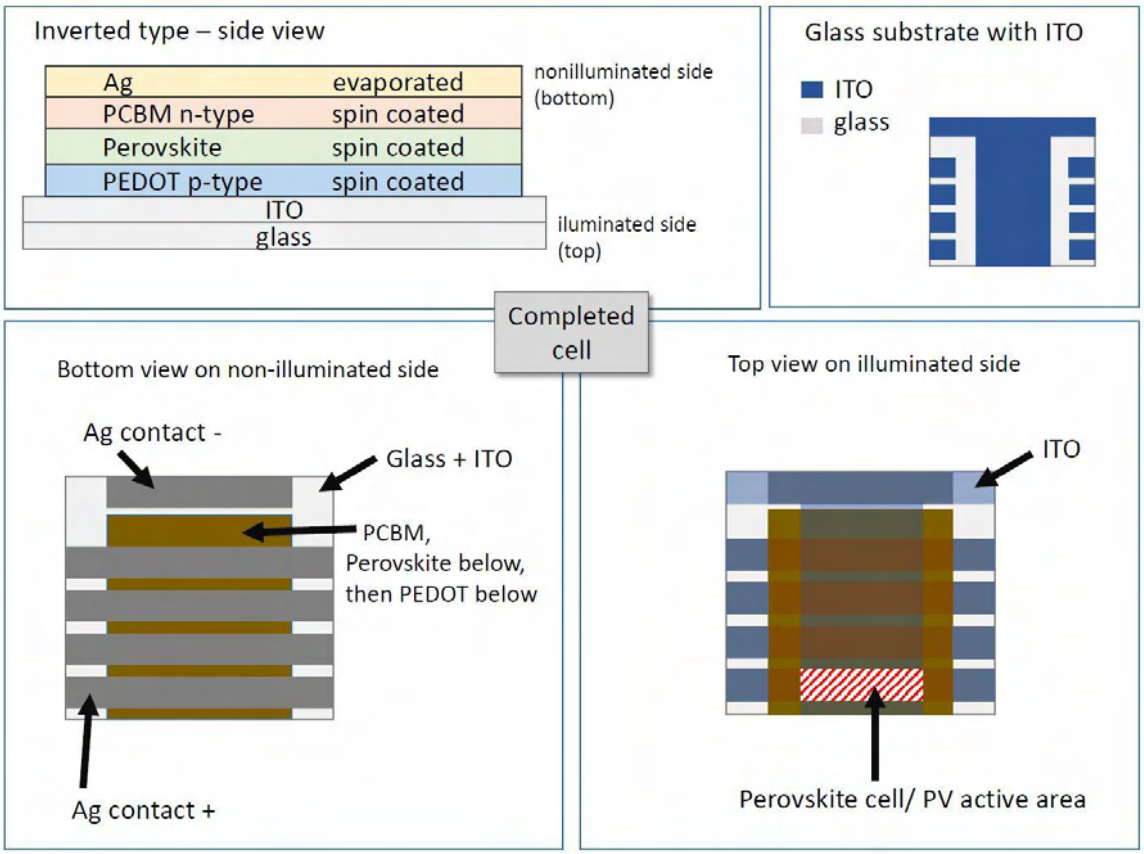

Figure 6: Schematic overview of inverted cell structure

The active cell area is the part of the substrate where all five layers overlap. As PCBM, Perovskite and PEDOT are covering most of the substrate, the positioning of silver and ITO defines the cell's size.

With a cell area of 0.3 cm^2 these devices are larger in comparison to many other groups (e.g. 0.06 cm^2 [31], 0.09 cm^2 [32], 0.126 cm^2 [33] and 0.16 cm^2 [34]). Even larger cells are needed for commercial applications. But large cells result in a higher likelihood for defects and therefore usually a worse performance. For fundamental research purposes in general and for this study in particular large cells are not favourable since the behaviour of the materials is investigated rather than the scalability of the fabrication process and the influence of fabrication defects would unnecessarily complicate the investigations.

Nine substrates were fabricated at once with four cells each.

Chemicals and devices in use

All chemicals and devices used are listed in the supplementary information in Table 6.

Cell fabrication procedure

In order to fabricate the cells the following procedure has been carried out:

I. Substrate is ultrasonic cleaned in detergent (Hellmanex) for 30 minutes and 50% power
II. Substrate is washed with demineralized water
III. Substrate is ultrasonic cleaned in demineralized water for 30 minutes and 50 % power
IV. Substrate is washed with Isopropanol and blow dried
V. Substrate is plasma cleaned for 2 hours
VI. PEDOT (Heraeus Clevios PVP.AI 4083) solution is filled into a syringe then a filter is attached to the syringe
VII. PEDOT is spun on top of the ITO for 30 seconds with 1500 rpm and 500 rpm/s in a laminar flow cabinet
VIII. Substrate is sat on hotplate at 200 °C for 5 minutes with the glass side down
IX. Substrate is given the chance to cool down roughly 15 minutes
X. A PCBM solution is prepared with $\frac{20\ mg\ PCBM}{ml\ Chlorobenzene}$ and left at 70 °C *
XI. A Perovskite solution is prepared with the following composition *

Pb(Oac)2	502.41 mg
MA-I	631.65 mg
DMF	1.802 ml

XII. The solutions and all substrates are transferred into a glovebox with nitrogen atmosphere and an O_2 level of roughly 20 ppm and a H_2O level of 30ppm

XIII. Perovskite is spun on top of PEDOT for 45 seconds at 2000 rpm and 2000 rpm/s

XIV. The substrate is immediately blow dried for 10 seconds then sat on a hotplate at 90 °C for 10 minutes

XV. After the substrate has cooled down PCBM is spun on top of the perovskite for 30 seconds at 3000 rpm and 2000 rpm/s

XVI. Deposited material is scratched off the substrate on the three contact sides in order to expose the contacts so that only the brown area shown in Figure 6 is left.

XVII. Silver is evaporated on top of the cell using a mask to get the pattern shown in Figure 6

XVIII. The substrate is sealed with glass glued on top of the silver using resin

* Both solutions should be made about 3 hours prior to the spin coating

3.2 MEASUREMENT OF ELECTRICAL PROPERTIES

Initial I-V curves

Initial I-V curves for the cell characterization were measured with the solar simulator. The procedure presented in the following, has been worked out to yield reproducible results with stable I-V curves for the investigated cells.

A masked cell is illuminated at room temperature, 24 (±2) °C. The cell is light soaked for 45 minutes. Voltage is applied to sweep through the curve and the resulting current and cell voltage values are measured (4 Probe) by a source meter and recorded via a LabView script.

The light source has been manufactured by Newport, model 91160A – 1000. An overview of the corresponding light spectrum is given in Figure 7. It meets the AM 1.5G spectrum defined in the standard testing conditions for terrestrial photovoltaic devices in the IEC60904-3 standard.

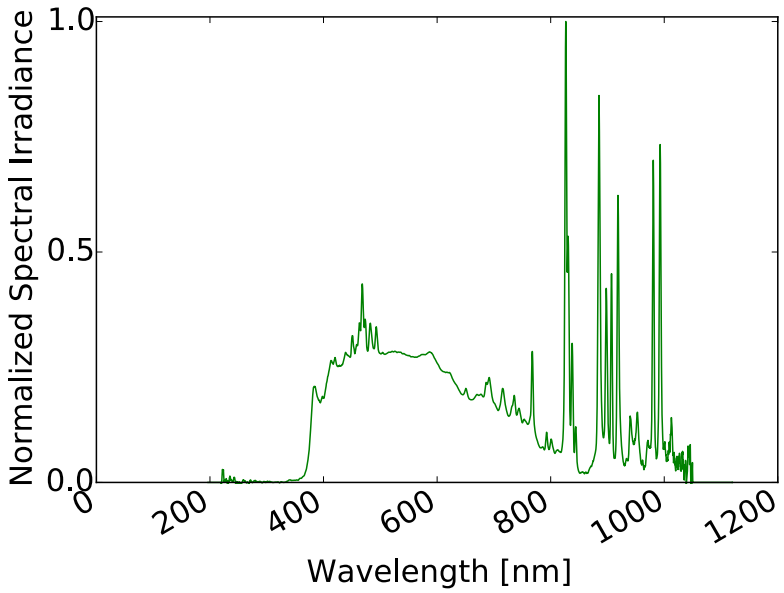

Figure 7: Emitted light spectrum of the Newport 91160 A- 1000

The source meter in usage is a Keithley, 2400 SMU.

The following parameters were used (note that start and end voltage are swapped for reverse scans):

- Wait time for each voltage step = 0.2 s
- Voltage step size = 20 mV
- Start voltage varies in the range of -0.2 V to 0 V
- End voltage varies in the range of 0.9 V to 1.2 V
- Irradiance = 1 sun

All cells were stored in a dry cabinet or the glove box with typical relative humidity levels of 3 % and 30 ppm, respectively (humidity levels fluctuate with the frequency of access).

For the measurement of I-V curves under different irradiance levels, light filters were applied to the light source with a transmittance of 0.74, 0.5, 0.25 and 0.1.

Transient and other measurements with the Paios system

For all transient measurements the Paios system manufactured by Fluxim was used.

Paios is a system designed for solar cells and OLEDs that provides a wide range different measurements types while maintaining the same measurement setup. Therefore the measurement resistances and contact resistances remain the same.

A circuit diagram is given in Figure 8 where the measurement's electrical setup is displayed.

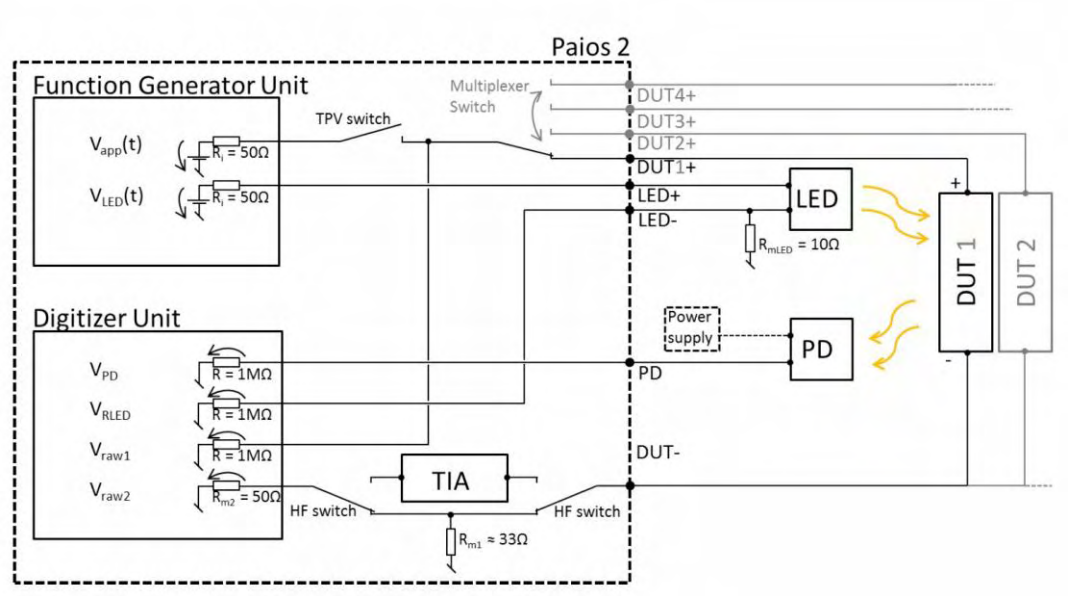

Figure 8: Electrical circuit diagram of Paios, taken from Paios user manual 3.1 by Fluxim AG

The Paios system is able to modulate the light intensity (modulation of LED current) and the applied voltage via a function generator unit. The probed devices are displayed in the electrical circuit diagram as DUT 1 and DUT 2. The LED's voltage (V_{RLED}), the device voltage (V_{raw1}) and the device current as a voltage drop over R_{m2} (V_{raw2}) are measured. Via opening the TPV switch the open circuit voltage of the device can be measured. The HF (high frequency) switch enables the Femto Trans-Impedance-Amplifier (TIA). The TIA amplifies very low currents with variable gains which might occur during transient, sequential I-V curve and impedance measurements. From

these measured voltage values, the known resistances and the impedance calibration data all further data is calculated.

Based on that setup various measurement techniques can be applied using the Paios software. That includes current voltage characteristics (I-V curves), transient photocurrent and photovoltage, CELIV (charge extraction by linearly increasing Voltage) and impedance spectroscopy measurements. In addition to these techniques, that are applicable via the Paios software, user defined techniques can be set up.

Most experiments were set up in the LabVIEW based Paios software as “user defined experiments”.

In the supplementary information the light and voltage modulation for the different experiments is presented for most experiments as shown in Table 2. The experiments name is listed first. A certain time step is defined as the basic time interval of which multiples can be called. Light level as well as the voltage level can be set for certain multiples of the basic time step. The setting remains valid until new conditions are defined in a new command line. Apparently an infinite amount of command lines and time steps are programable.

Experiment name	**Time step [s]**	**60**
Time [s]	**Voltage [V]**	**Light level [%]**
Time step × Value1	Value1	Value1
Time step × Value2	Value2	Value2
…	…	…

Table 1 Sample experiment setup

The light spectrum of Paios measured by the manufacturer is displayed in Figure 9.

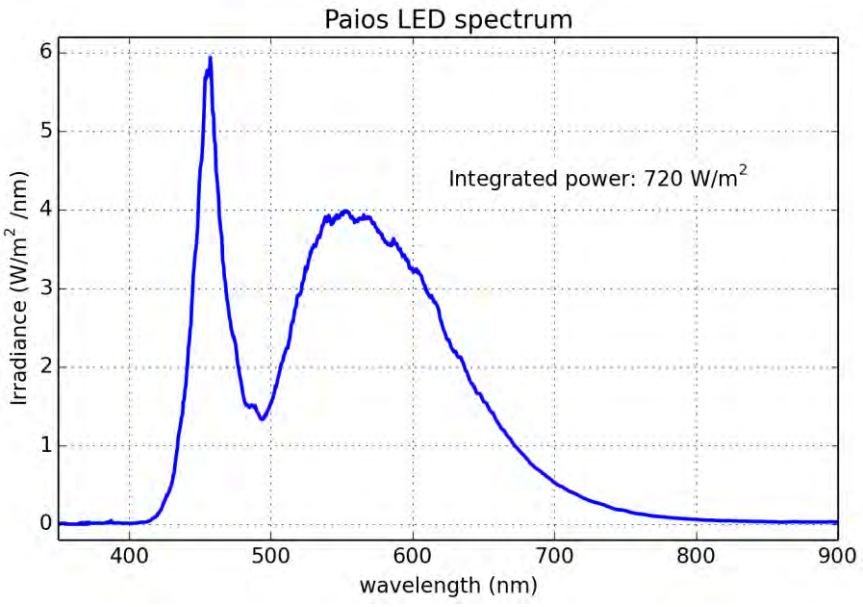

Figure 9: LED spectrum of Paios system provided by Martin Neukom, Fluxim AG

Paios' irradiance intensity for 100 % illumination has been measured to be 3.8 suns and shows a linear behaviour if scaled down.

With the initial understanding that 100 % would equal roughly 1 sun that measurement has been carried out after several tests have already been done. Therefore a 100% light level is used in some tests. After discovering that fact experiments were mostly carried out under 20 % or 25 % illumination.

We assume to have an equivalent intensity of roughly 1 sun for 25% illumination. If results for Paios measurements are shown in the following, claiming to have been carried out under 1 sun condition, its referring to the conditions stated above.

Calibrating the Paios irradiance, no correction for the different irradiance spectra was made.

The relevant absorption range of $CH_3NH_3PbI_3$ is roughly between 300 and 800 nm. The spectrum of the solar simulator spans over a range from about 350 to 1050 nm with distinct spikes between 800 and 1050 nm. Most of these spikes should not affect the cell as its absorption range ends around 800 nm. However the solar simulator's spike (roughly at 820 nm) on the edge to the cell's absorption range shown in Figure 3 might clearly influence cells with slightly higher absorption ranges (imagine the absorption range ends a) at 800 nm or b) at 830 nm). The spectrum of the Paios (about 410 to 750 nm) is not as broad as the solar simulator's spectrum with a groove from 470 to 530 nm. Effects within the cell occurring due to wavelengths of that range will be missed out but no peaks around the absorption range's edges are observed.

Light soak

Often it has been observed that the cell's performance improves if left under continuous illumination for certain time periods spanning from 15 minutes up to two hours.

This procedure is referred to as light soak.

Curve fit

The single exponential curve fits to the transient current decay in order to obtain the τ value were done via applying the least square method and the following model

$$f(t) = B + A_1(e^{-\frac{t}{\tau_1}})$$

It is used for silicon, dye and perovskite cells. If in future reliable data for the perovskite cells was acquired the following double exponential fit might be taken into consideration

$$f(t) = B + A_1(e^{-\frac{t}{\tau_1}}) + A_2(e^{-\frac{t}{\tau_2}})$$

3.3 ACTIVATION ENERGY

The activation energy, E_a, is the energy level ions have to overcome in order to leave the atomic lattice. Higher activation energies indicate a lower likelihood for ions to break free.

Trying to understand whether ionic movement influences the current, a closer look at the activation energy of the cells is worthwhile as it might bear valuable information about the presence of ions.

In order to experimentally obtain the activation energy an already light soaked cell is, whilst illuminated, exposed to a voltage step. The transient current response is measured at different temperatures and the τ value for the current stabilisation is obtained.

Plotting the logarithm of inverse τ vs the inverse of temperature, ideally a line can be fit to the data with the slope s as seen in Figure 10.

Derived from the Arrenhius equation the activation energy can be calculated by:

$$\mathrm{E}_a = -\mathrm{slope} \times \mathrm{k}_b \ \left[\frac{\mathrm{kg\,m^2}}{\mathrm{s^2}}\right]$$

With Boltzmann constant, k_b = 1.38064852 $\times 10^{-23}$ $\left[\frac{\mathrm{kg\,m^2}}{\mathrm{s^2 K}}\right]$ and the slope, s in [K] and can be converted in electron volts with 1 eV = 1.60217653$\times 10^{-19}$ $\left[\frac{\mathrm{s^2}}{\mathrm{kg\,m^2}}\right]$.

For this calculation the data from the “Voltage steps of different sizes #1” experiment were used.

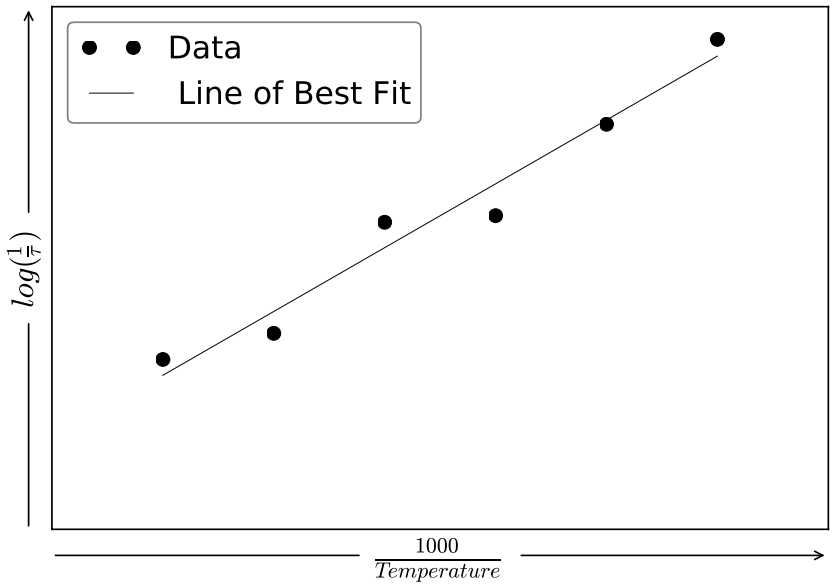

Figure 10: Exemplary visualization of the straight line fitting to experimentally obtained data

To obtain the τ values a two exponential curve with the function:

$$f(t) = B + A_1(e^{-\frac{t}{\tau_1}}) + A_2(e^{-\frac{t}{\tau_2}})$$

is numerically fit to the data with the least square fit method.

An averaged τ value is obtained by applying the weighted arithmetic mean:

$$\tau = \frac{\tau_1 \times A_1 + \tau_2 \times A_2}{A_1 + A_2}$$

4 EXPERIMENTS AND RESULTS

4.1 CELL FABRICATION

During the early cell fabrication, different parameters were identified that influenced the performance of the cells. These empirical findings of the cell production process are briefly summarized in the following.

- Exposure to air for short times (no more than 1 or 2 hours) seems to improve the cells fill factor and efficiency.
- A performance optimum seems to be located around rotational speeds of 2000 rpm for spin coating of the perovskite layer (resulting in a specific thickness of the perovskite layer, which has not been measured so far).
- Deposited, to the eye uniform occurring layers perform well, but non uniform looking layers do not necessarily perform worse.
- Even if kept under nitrogen atmosphere perovskite solution seems to age. Cells fabricated with aged (several days up to weeks old) perovskite solution perform worse.

4.2 THE THREE CELLS

The results presented in the following were mainly obtained for 3 different inverted structure type cells. These particular cells were chosen as they show only very little hysteresis in the initial I-V scan. The W-7-6.1 cell was fabricated by the author at CSIRO. OP 10 and OP 7 were fabricated by a member of the group lead by Prof. Snaith, University of Oxford.

cell name	η [%]	V_{oc} [V]	I_{sc} [mA]	FF	area [cm^2]	material
W-7-6.1	6	0.83	3.9	0.56	0.3	$MAPbI_3$
OP 10	9.7	1	2.4	0.66	0.17	?
OP 7	7.9	0.98	2.1	0.63	0.18	?

Table 2: Overview of three investigated inverted structure perovskite cells

Both OP cells are on the same substrate and hence fabricated the same way, which is so far unknown to the author. The W-7-6.1 cell, in the following referred to as “W” cell, was fabricated as explained in chapter 3. With the same procedure non encapsulated devices with higher efficiencies up to 10.5 % were fabricated in a reproducible way but unfortunately degraded before further testing could be done. Four I-V curves of these cells are shown in Figure 11 as an example of their performance. A hysteresis can be observed but is low compared to the hysteresis

of differently structured devices. Due to an unresolved issue in the laboratory, these results could lately not be reproduced.

It should be noted that in the course of this work, some results may not match the results of the initial I-V curve scan. That is due to the degradation of the cell over time and most likely due to the different light sources in use (solar simulator and Paios). Measurements with the Paios system were carried out in order to determine trends, not absolute values. Unfortunately, at some point, the W cell (and all cells of the same batch) got destructed by an overheating of the dry cabinet, leaving some open questions. The circumstances did not allow the fabrication of new cells.

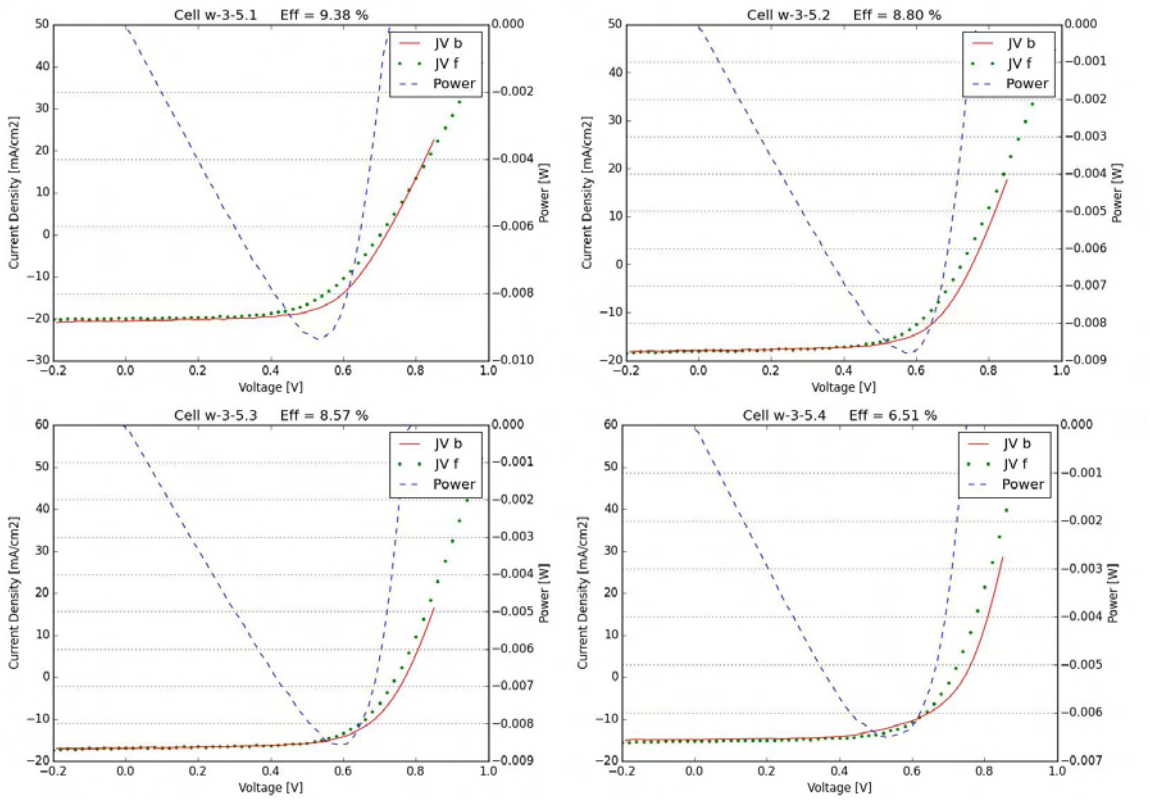

Figure 11: Examples for I-V curves of inverted structure $MAPbI_3$ cells fabricated by Walied Moustafa at CSIRO, the power curve refers to the backward scan

Standard I-V curve measured under the solar simulator with long like soak and dwell times grant a first impression of the cells performance before further experiments are conducted.

All three cells (W, OP 7 and OP 10) were measured before further testing was conducted. The I-V curves are displayed in Figure 12, Figure 13 and Figure 14. It should be noted that all show very little hysteresis. Whereas OP 10 has a V_{oc} of 1 V and a reasonable fill factor, cell W has both a lower V_{oc} and a lower fill factor. The current of OP 10 is lower than W's current, but it has to be taken in consideration that OP 10's cell area is significantly smaller. OP 7's parameters are slightly worse than OP 10's but better than W's.

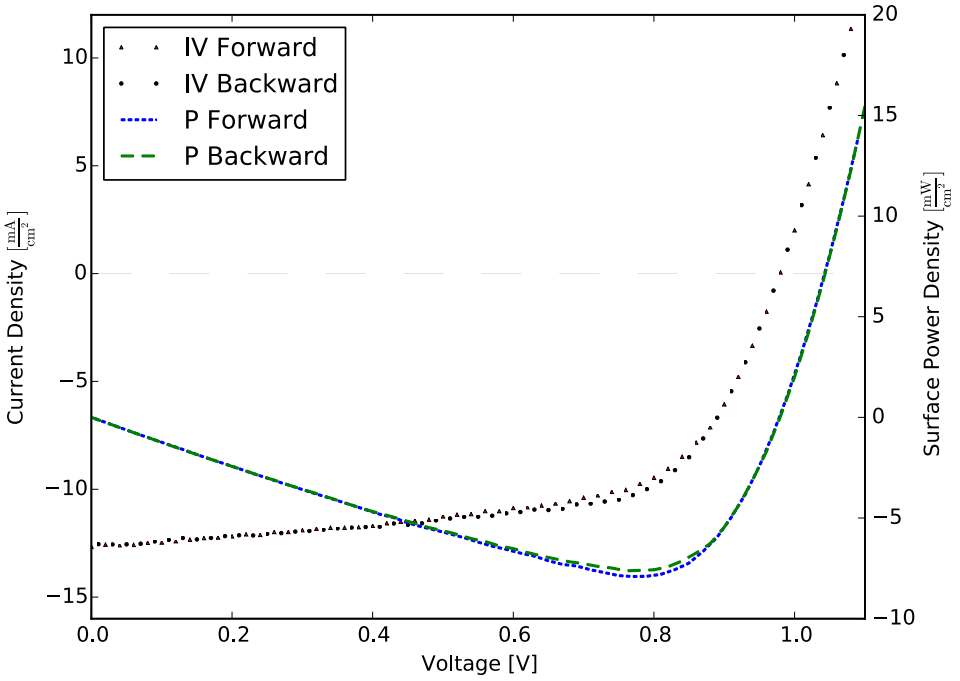

Figure 12: Initial J-V curve of OP 7 at 25 ℃, 1 sun and 45 minutes light soak

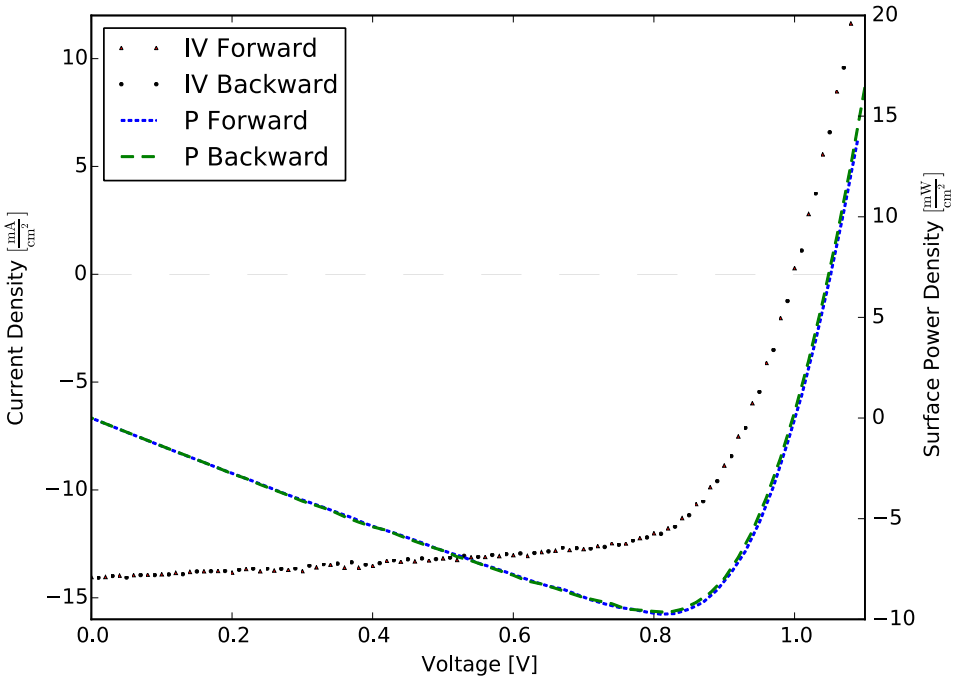

Figure 13: OP 10 cell initial J-V curve at 25 ℃, 1 sun and 45 minutes light soak

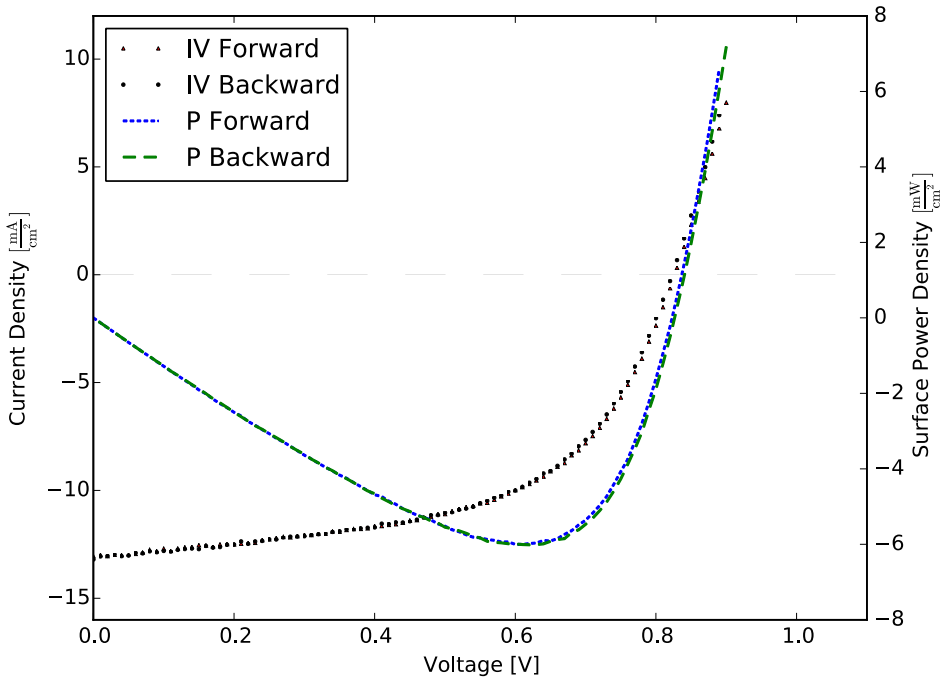

Figure 14: Initial J-V curve of the W-7-6.1 cell at 25 °C, 1 sun and 45 minutes light soak

The I-V curves measured after testing the cells for 2.5 (W cell) and 1 month (OP 10 and OP 7) are displayed in the supplementary information section. W's and OP 10's Voc and Isc values decreased whereas OP 7's I-V curve meets the initial curve well. OP 7 has undergone far less testing than the other two cells which might be the reason that no change is observed.

It is noted that additionally a hysteresis occurs for W and even more distinct for OP 10.

4.3 MEASUREMENT AND CALCULATION OF T FOR THE DWELL TIME ESTIMATION

Voltage steps through I-V curve

The aim of this experiment is to gather information about the transient behaviour of the cell's current and, based on the results, obtain τ values.

This experiment is an I-V measurement with a certain voltage step size and long dwell time. The current is measured at specific voltages which are stepwise increased by 10 mV a hundred times (from 0 to 1 V) and being hold for a certain dwell time. This experiment is carried out under 100 % Paios illumination (3.8 suns) and with a steady room temperature of 20 °C but not with an additional temperature stabilization of the cell.

The current's behaviour, as a result of this experiment, is visualized in Figure 15 where the transient current response to each change of the voltage is shown (as observed for a dye cell, other cell types might display different transients).

It can be observed that for each voltage step (or cell voltage change) the current signal takes a certain time to stabilize. An immediate current measurement would result in a lower current value (and hence a lower cell performance) than a measurement taken at some point later on.

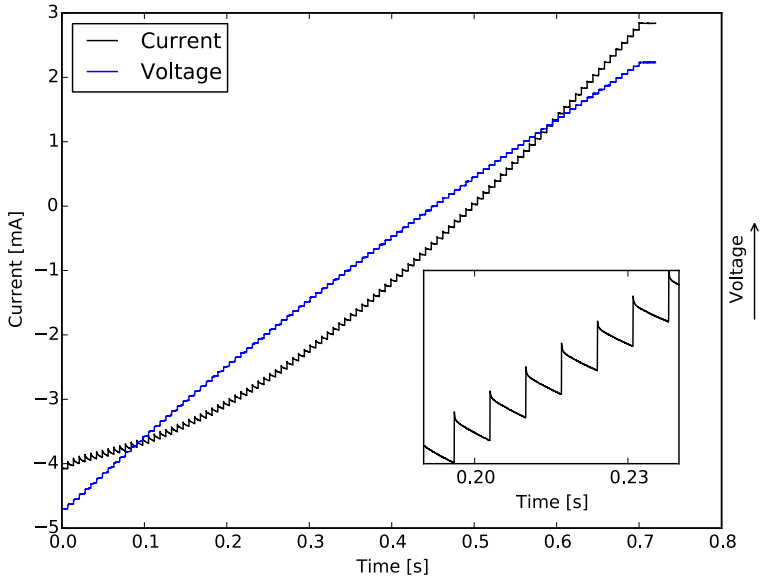

Figure 15: Liquid junction dye cell, transient current response to stepping 100 steps each 10 mV (from 0 to 1 V) through I-V curve with detailed view of the time range of 0.19 up to 0.24 seconds

To obtain the τ values and hence estimate the necessary dwell times, transient measurements of the current behaviour due to voltage steps through the I-V curve were performed and curves were fit to each decay. This experiment was conducted using a liquid junction dye sensitized cell

as this cell type is already much better investigated than Perovskites but responding slower than silicon cells.

As it can be seen in an excerpt of the whole I-V curve in

Figure 16, the obtained τ values differ slightly (from 2.5 ms to 5 ms) increasing with increasing voltage for this cell. To achieve best results for the cell's performance the highest τ has to be considered and therefore all τ for each voltage range should be calculated.

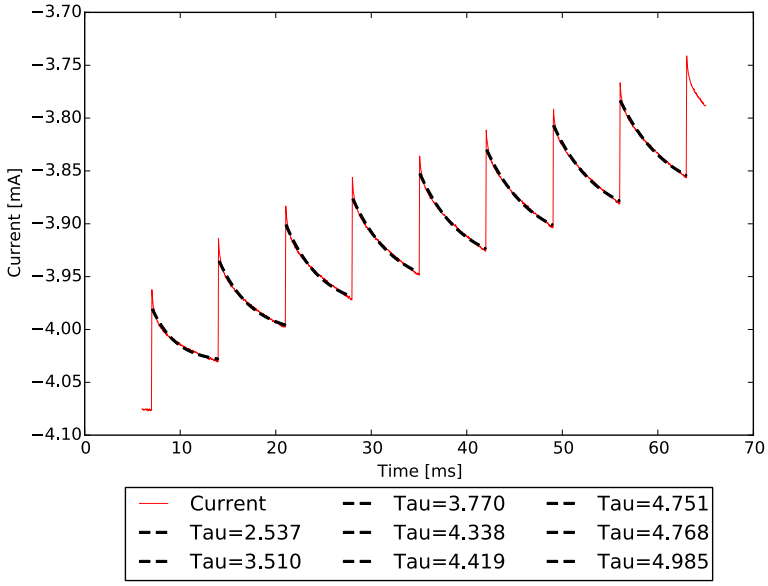

Figure 16: Illuminated liquid junction dye cell, excerpt of stepping up the I-V curve with 10 mV steps and a curve fit for each step with the obtained τ values

That has been successfully done for a silicon photodiode and the dye cell and is displayed in Figure 17. A very equal distribution for the silicon diode can be observed up to 600 mV then the values become scattered. For the dye cell a trend can be observed with higher τ values in the range of 0 to 400 mV and a diminishing τ from 400 mV to 1 V. For the inverted structure perovskite cell (not the W cell but a copy fabricated the same way) all values seem to be quite scattered. The relaxation time after each voltage step is too long for Paios' high resolution transient measurements and hence can't be measured that way. Unfortunately it is too fast for the lower resolution range (resulting in approximately 8-10 measurement points per second). With Paios automatically choosing the low resolution measurement for the long testing period of Perovskite (300 s) only few data points for a single transient decay are obtained. The amount of measured

data points (often 2 – 5 points) is simply not high enough to confidently perform a curve fit and obtain a trustable τ value.

I-V curves with different τ values as dwell times

The aim of this experiment is the confirmation of adequacy of the proposed dwell time estimation method.

This is not a user defined experiment but one of the standard I-V curve measurement procedures provided by Paios. The Paios sequential I-V measurement method is applied with different multiples of the obtained τ value as dwell times at a steady room temperature of 20 °C but without an additional temperature stabilization of the cell.

The dwell time (in the Paios software called waiting time) for each voltage step is [0.5, 0.75, 1, 1.25, 1.5, 1.75, 2, 2.5, 3, 3.5, 4, 4.5, 5,10] × τ, with a voltage step size of 10 mV, a start voltage of -0.1 V, an end voltage of 0.9 V as well as an illumination of 100 % (3.8 suns).

With the maximum τ value of 20.51 ms for the Dye Cell an I-V curve scan with different dwell times was performed. Indeed as it can be seen in Figure 18 the cell's performance improves with a dwell time of 3 τ compared to 1 τ. Best results are achieved for 5 τ but no further improvement

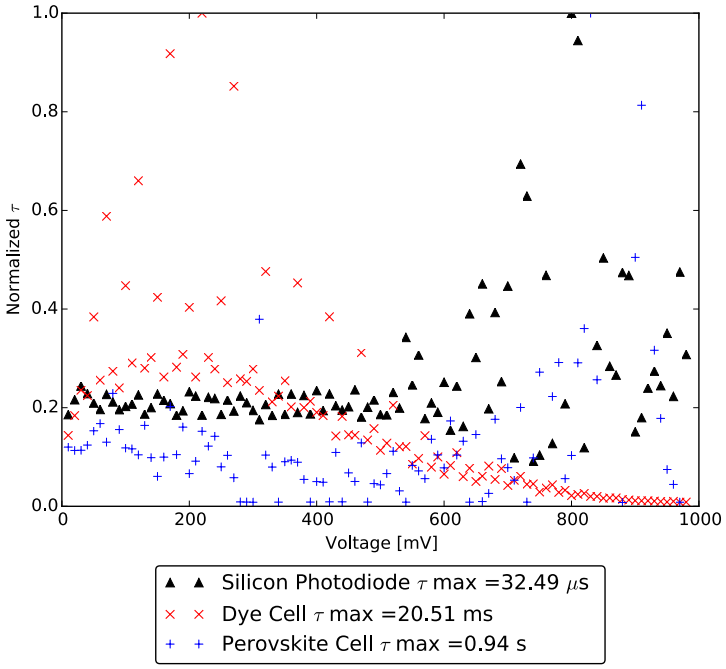

Figure 17: τ values obtained in different voltage ranges of the I-V curve for a silicon photodiode, a dye cell and a perovskite cell, τ normalized over the maximum obtained τ

can be observed for 10 τ. This experiment has been carried out a second time with a higher variety of dwell times but four month later than the first experiment under an illumination of 25% instead of 100%. The same trend is observed even under a different illumination (the cell degraded slightly, I_{sc} ≈ 0.8 mA at 25 % illumination compared to ≈4 mA at 100 % illumination). For small τ values a huge change in the I-V curves can be observed while differences between higher τ almost vanish completely as it can be seen in Figure 18. Unfortunately these graphs cannot be produced for the silicon photo diode since the provided equipment is not able to measure with dwell times as fast as 30 µs (fastest 10 ms). Therefore the 5 τ limit is always exceeded by far.

The results and τ values for this "Voltage steps through I-V curve "measurement were not reproducible. That can be accounted to the imprecise measurement at low time resolution but it can't be the only explanation for the observed variation of results. Another effect that was discovered in that study (memory effect) and will be discussed later on, is most probably responsible for the non-reproducibility.

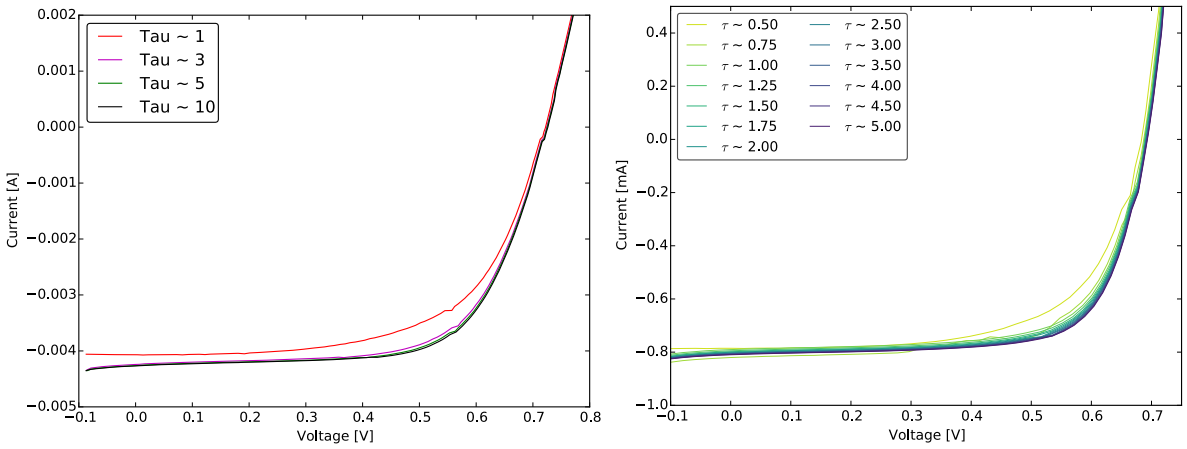

Figure 18: Forward I-V curves of the dye cell measured with several dwell times equal to certain τ values. In the left diagram the curves were measured the same week as the transients but only 4 different dwell times have been investigated. The right diagram shows more curves for more dwell times, but the measurements were taken about 4 months later and the cell already degraded

Prior to the memory effect the influence of physical parameters such as light level, light soak and temperature will be discussed in the following.

4.4 TEMPERATURE AND LIGHT LEVEL INFLUENCE

It is important to gain an understanding of how the cells are responding to changes in light or temperature before trying to understand the driving forces behind the measurement problems.

In the following temperature and light influences are discussed and it is found that they strongly influence the cell's performance.

I_{sc}, V_{oc} and fill factor dependency on temperature

This experiment aims on analysing the cell's behaviour towards temperature influence.

This experiment is not set up as a user defined experiment. The I-V curve sequential measurement function with a 20 mV Voltage sweep rate, a fixed 200 ms waiting time at each voltage step, a light intensity of 25% and a measurement range of -0.2 V up to 1.2 V is manually started. It does take 3 measurements at each voltage step and averages the result.

The cell is placed in the cryostat, brought to a low temperature of roughly - 12 °C and is then light soaked for 50 minutes. Then a forward and reverse I-V scan is performed. The temperature is gradually stepped up and as soon as the cells current is stable the next set of I-V curves is measured. This process is repeated until a temperature of roughly 30 °C is reached

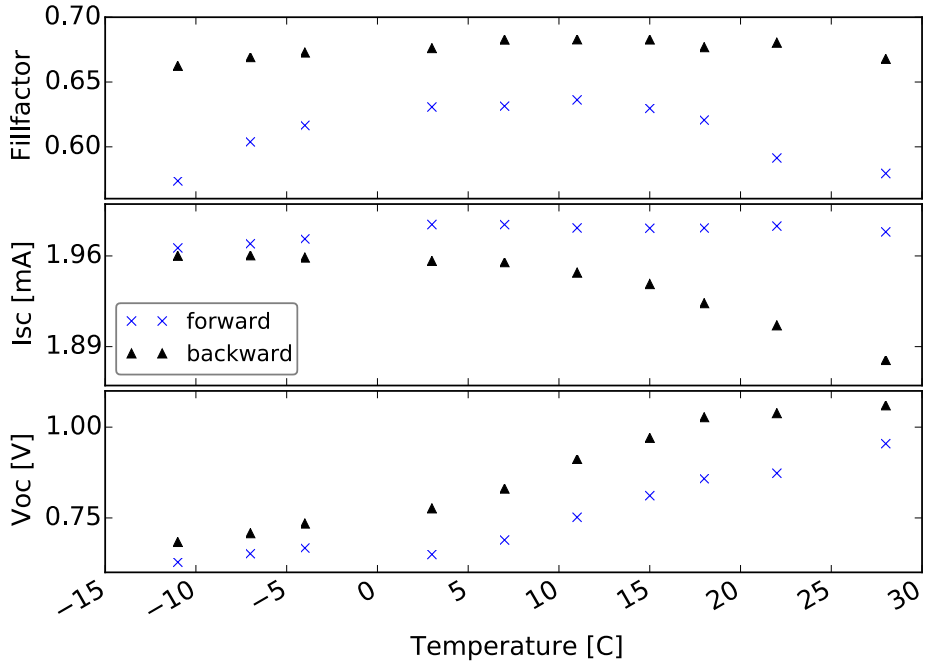

Figure 19: Temperature dependency of OP 10

Carrying that experiment out and investigating the temperature influence on the cells (in Figure 19, Figure 20 and Figure 21, forward and backward I-V scan results are shown) it can be observed that both OP cells behave similar but opposite to cell W. Both the fill factor and the V_{oc} appear to be highly temperature dependant.

Whereas V_{oc} distinctly rises for OP 10 in a temperature range of about – 15 °C to 30 °C ($\Delta V_{oc} \approx 0.4$ V) and OP7 ($\Delta V_{oc} \approx 0.5$ V) it drops for W ($\Delta V_{oc} \approx 0.2$ V) with an increase of temperature. The current marginally decreases for the OP 10 ($\Delta I_{sc} \approx 0.07$ mA) and OP7 ($\Delta I_{sc} \approx 0.03$ mA) backward scan and rises for W in both scan directions ($\Delta I_{sc} \approx 0.6$ mA) and when forward scanning OP 10 and OP 7 ($\Delta I_{sc} \approx 0.01$ mA).

The fill factor changes over the temperature range. It increases for the W cell with rising temperature and has an optimum around 10 °C for the OP cells.

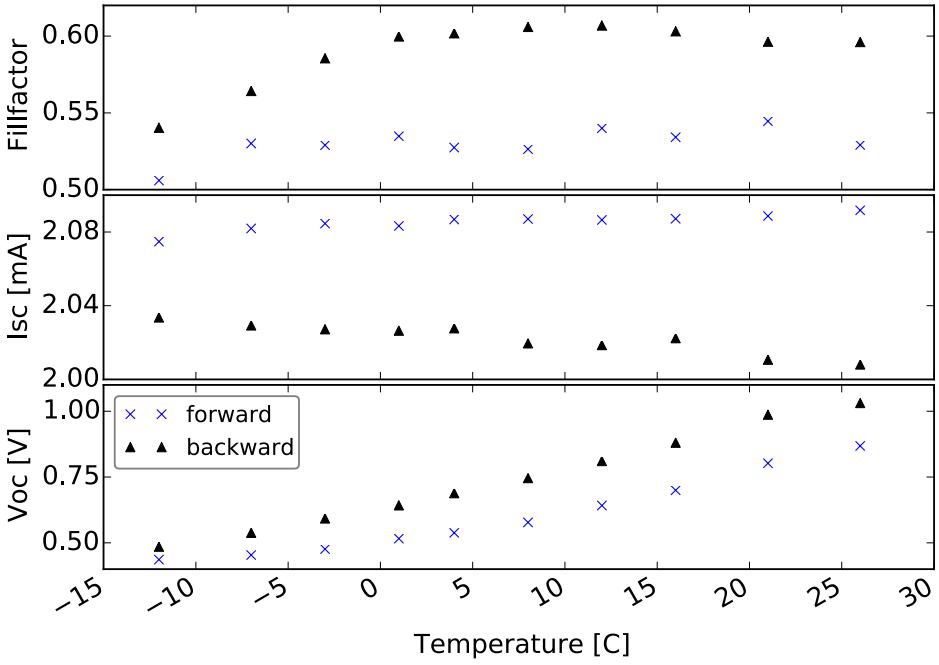

Figure 20: Temperature dependency of OP 7

A huge difference considering the fill factors depending on the scan direction can be observed for OP 10 and OP 7. As Figure 22 indicates, the difference for the forward and reverse scan fill factors for the W cell are much smaller. The trend is mostly consistent with the final solar simulator I-V curve measurement performed after running all other tests discussed in this study (Figure 45, Figure 46 and Figure 47 in the supplementary information) where a slight hysteresis for the W cell and a larger hysteresis for the OP 10 cell is observed.

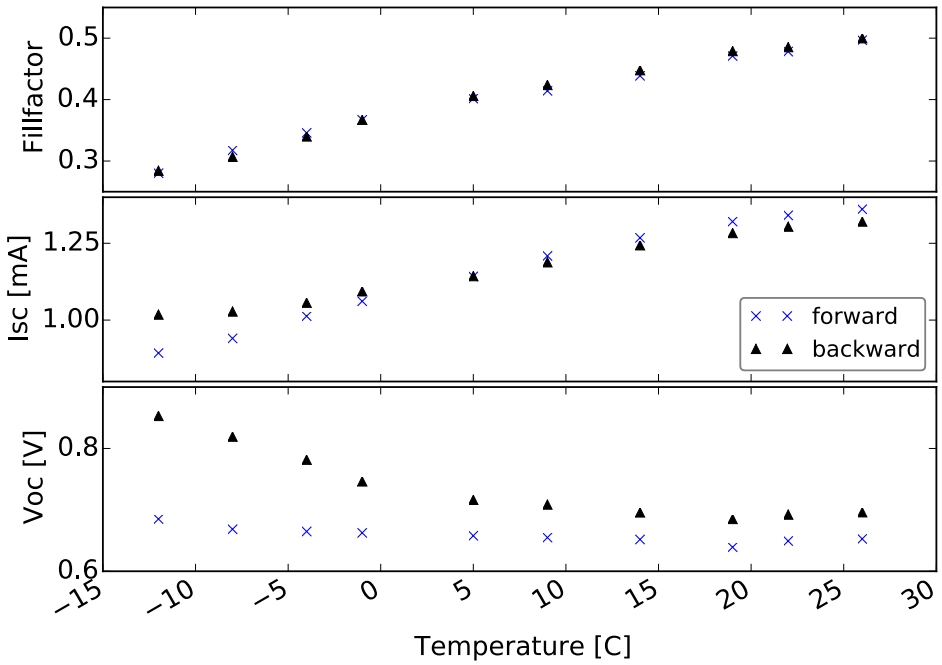

Figure 21: Temperature dependency of W-7-6.1

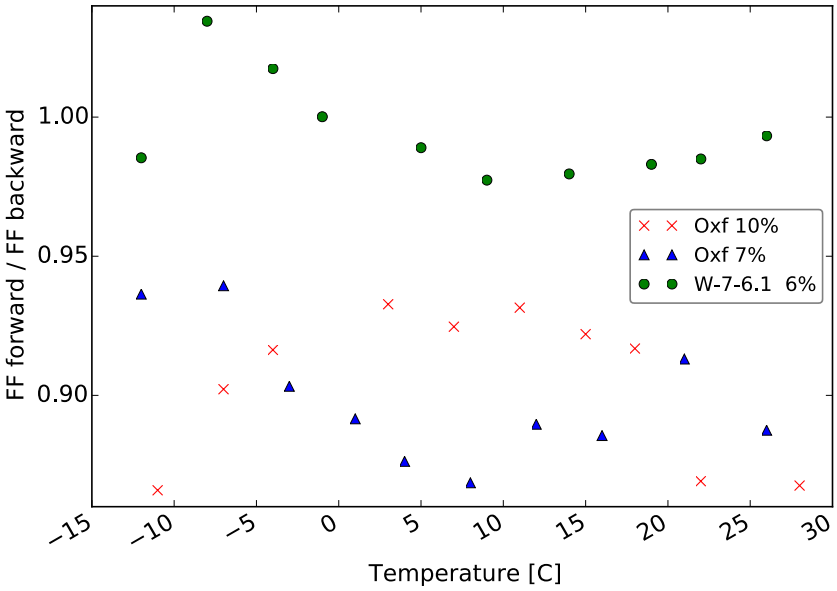

Figure 22: Ratio of forward and reverse fill factors over temperature

Dependency on irradiance level

With that experiment the influence of the irradiance level on the cell parameters are studied. The cell's I-V curve are measured with the solar simulator after a light soak (1 sun) of 45 minutes for different irradiance levels. Different light filters with a transmittance of 0.74, 0.5, 0.25 and 0.1 were applied to the light source to realize the different irradiance levels.

Measurements for more than one sun could not be performed, as the solar simulator does not provide that possibility. With the Paios spectrum not meeting the AM 1.5G spectrum, the Paios system was not used for this experiment.

Investigating the light level's influence a linear correlation between I_{sc} and the light level can be observed for our investigated range of 0.1 to 1 sun (results for OP 10 are shown in). That linear correlation is also valid for the maximum power point. The higher the irradiance level, the higher the short circuit current and maximum power point.

It is not quite clear what the appearing hysteresis for a light intensity of one sun can be attributed to. But it is causing the difference in the slope of both linear fits to the power, as the forward I-V curve's maximum power point is much lower (0.15 mW) than the backward measured one.

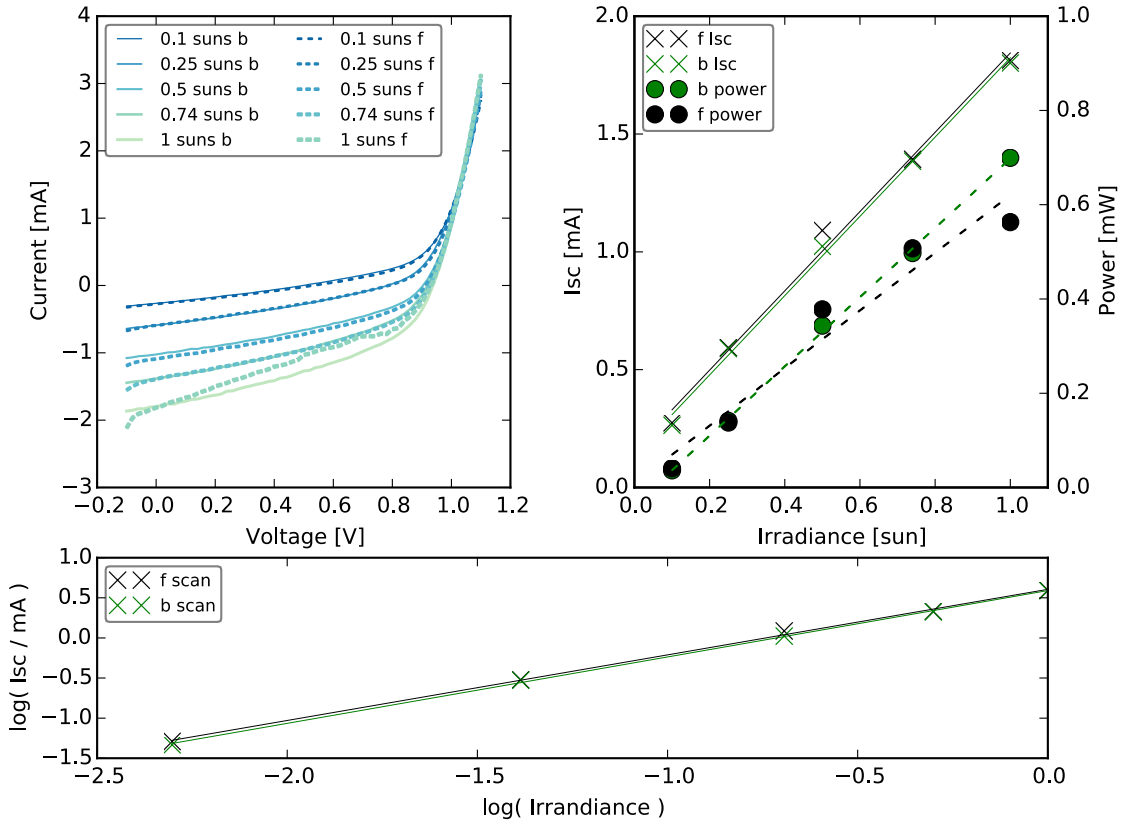

Figure 23: OP 10, effect of different irradiance levels on forward and backward I-V scan (top left) a linear dependency for short circuit current and maximum power point can be observed (top right)

4.5 ACTIVATION ENERGIES

Voltage steps of different sizes

The aim is to understand transient behaviour depending on temperature and gather data in order to calculate the activation energy.

This experiment is performed at different temperatures (-10 °C, 0°C, 10°C and 25 °C). Applying different voltage steps of different magnitudes to the cell should reveal the transient current behaviour, depending on the voltage step up rate through the I-V curve and temperature dependency.

From the current's transient response to voltage steps at different temperatures the activation energies are calculated according to chapter 3.3 (and from transient current data seen in Figure 24) for W and OP 10 and shown in Table 4 and Table 3. The values are derived from the obtained slopes of line fits to the τ values (seen in Figure 27 and Figure 25) and differ depending on the voltage step size.

OP 10 Cell	
Step size [mV]	Activation Energy [eV]
10	-0.098
25	-0.087
50	0.227
100	-0.115

Table 4: Activation energy for the OP 10 cell in eV depending on the step size

W-7-6.1 Cell	
Step size [mV]	Activation Energy [eV]
10	0.388
25	0.460
50	0.614
100	0.505

Table 3 Activation energy for the W cell in eV depending on the step size

The magnitude of the applied voltage step does influence the transient response. In general it can be said that the higher the step, the longer it takes the current to reach a constant signal. The higher the temperature the faster the current becomes constant.

Unfortunately the transients for the W cell were measured only once. One τ value (10 mV and 298 K) could not be properly calculated because the measured current is almost a straight line and therefore the exponential model does not apply.

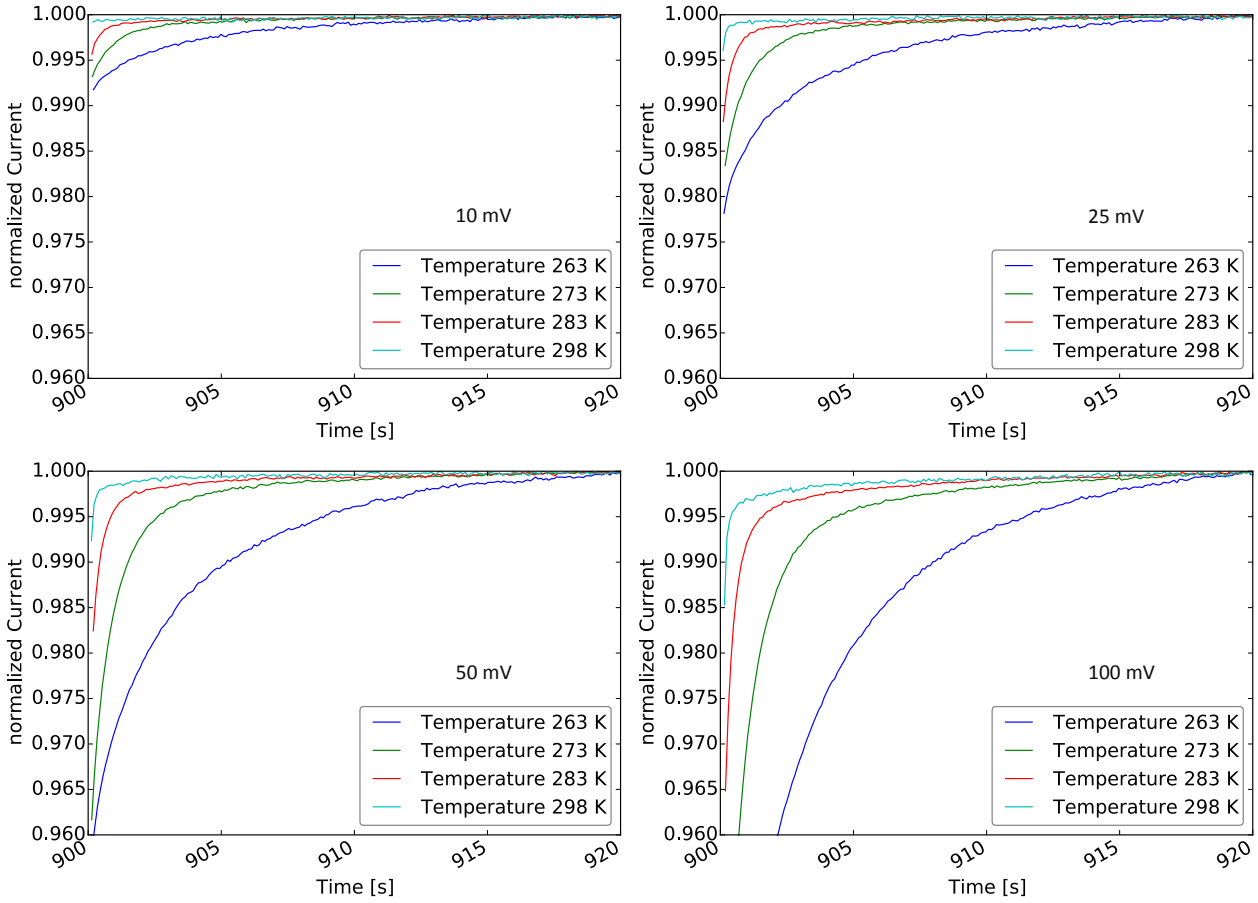

Figure 24: Different voltage step sizes (10, 25, 50, 100 mV) at different temperatures for cell W-7-6.1, data used to calculate activation energies

The values for the OP 10 cell are averages of 5 measurements. The W cell's values are varying between roughly 0.4 and 0.6 eV and are a bit higher than Meloni et al.[27] findings.

OP 10 shows negative activation energies. Negative activation energies are without any value except for indicating that the model the calculation is based on does not apply. Therefore it is concluded that other effects contribute much more to the cell's behaviour than ions.

One single τ value (265 K) causes the positive activation energy for the 50 mV step. Not taking that value into consideration a level of -0.154 eV would be obtained. Hence it is assumed that the activation energies for the cell are in general negative.

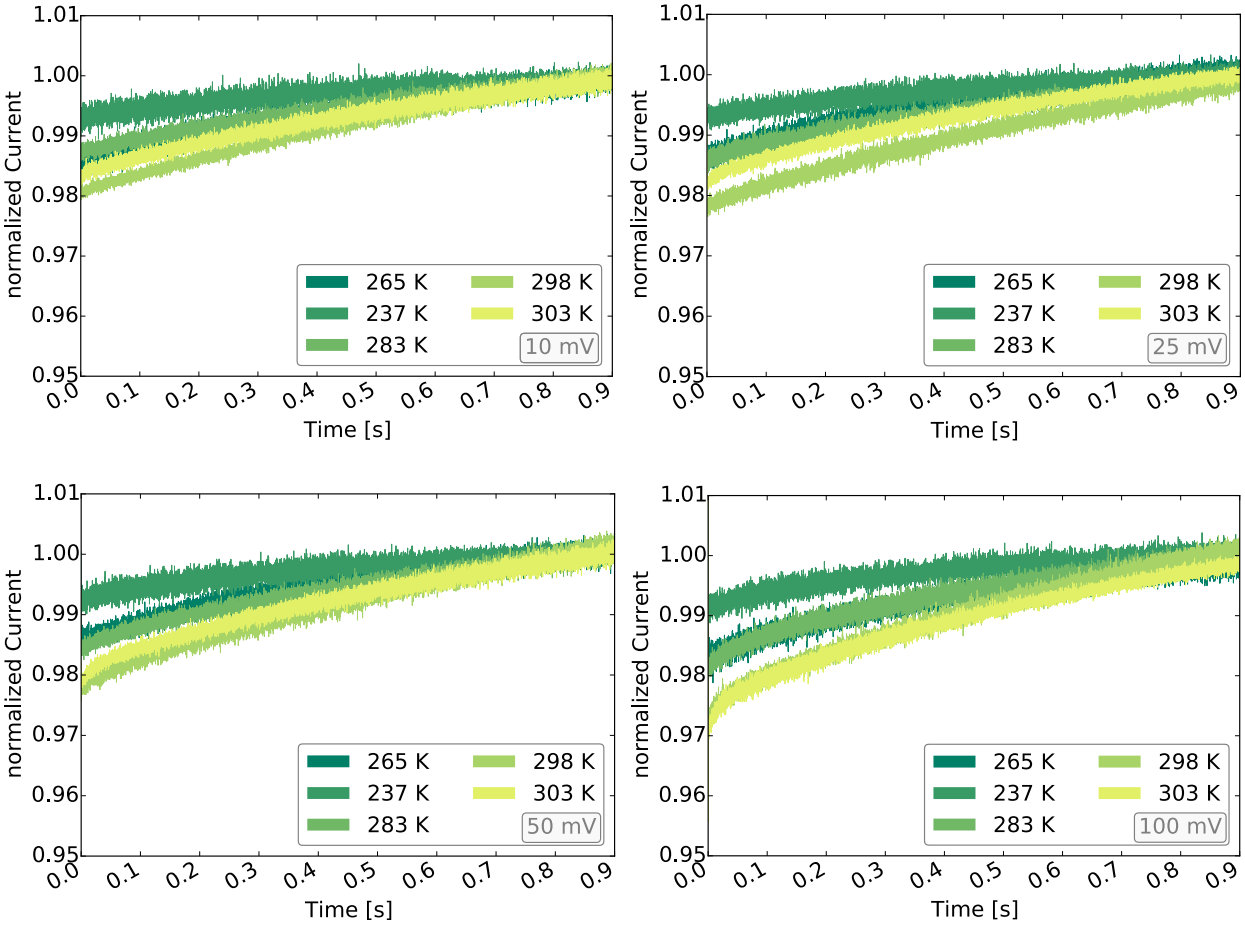

Figure 26: Different voltage step sizes (10, 25, 50, 100 mV) at different temperatures for cell OP 10, data used to calculate activation energies

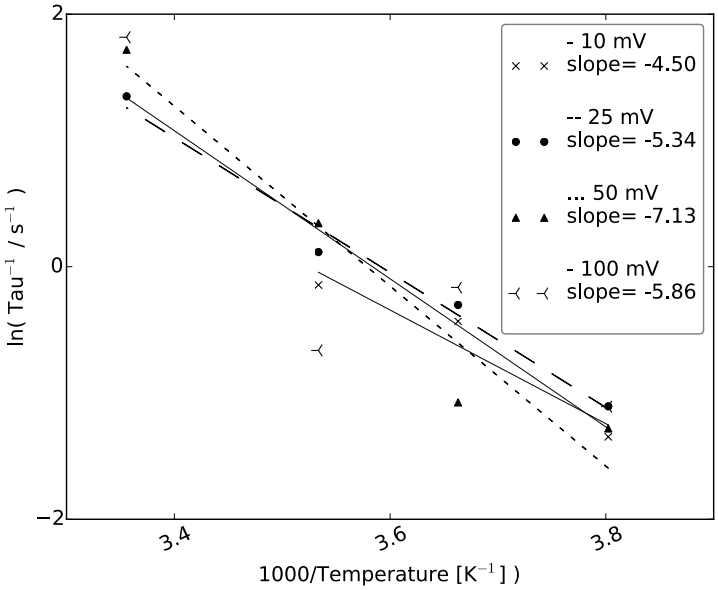

Figure 25: Logarithm of temperature plotted vs logarithm of τ to calculate activation energies for W-7-6.1 Cell

The difference of the activation energies for both cells are remarkable. Not only do they differ in the magnitude but one is positive and the other one is negative. That might be an explanation for the very different stabilization times and occurring effects during light soak as it can be seen later on.

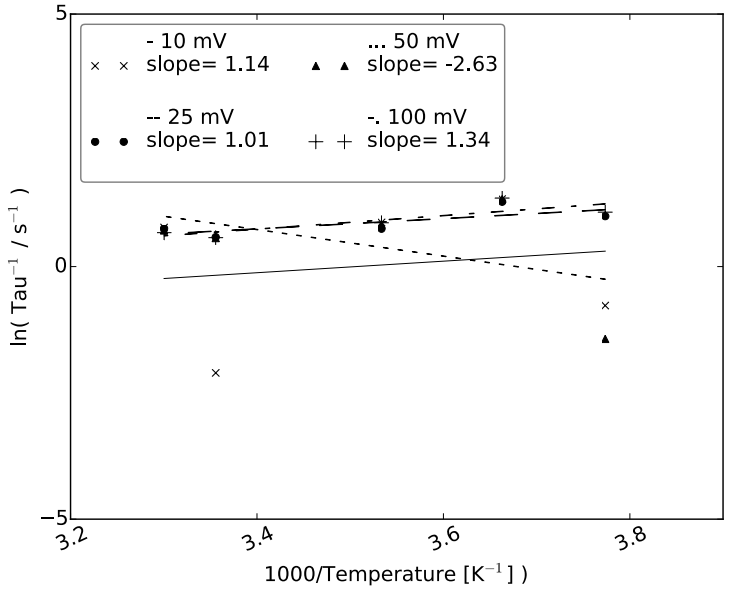

Figure 27: Logarithm of temperature plotted vs logarithm of τ to calculate activation energies for OP 10 Cell

4.6 LIGHT SOAK INFLUENCE

Measuring I-V curves it is obvious that the light soak has a big influence. Understanding what it exactly does is advantageous for all measurements.

Light soak and I-V measurements

The cell is light soaked with a stable temperature of 25 °C and I-V curves (forward scan) are recorded in 5 minute intervals, the measurement takes about 2.5 minutes with an absolute illumination time of 7.5 minutes between each measurement. After 75 minutes (10 measurements) the cell is given 60 minutes in the dark to relax. This procedure is repeated several consecutive times. To investigate the memory effect it is left in short circuit in the dark for different amounts of time to recover. Time intervals between two light soak experiments were 12, 6 and 3 hours.

With this massive impact of temperature and light level, all experiments were carried out under very stable temperature conditions (red line in Figure 28 indicates the sample temperature) using a cryostat (with nitrogen atmosphere) and a stable LED light source in Paios.

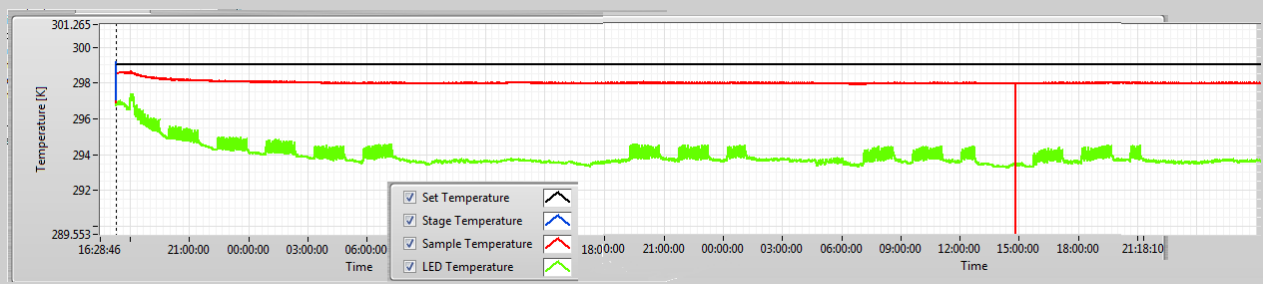

Figure 28: Temperature stability during the experiment

A cell was light soaked and I-V curves were measured every 5 minutes. It impacts the cell's V_{oc}, fill factor and hence the power, as it can be seen for OP 10 in Figure 29 (impact on I_{sc} is marginal). The longer the light soak lasts, the more all of the properties improve. After a rapid improvement in the first 20 minutes of illumination, the cell's properties are much slower enhanced. It can be observed that the cells power rises from 0.3 mW up to 0.52 mW (V_{oc} from 0.4 V up to 0.65 V) in the first 20 minutes and from 0.52 mW to roughly 0.6 mW (V_{oc} from 0.65 V up to 0.7 V) in the next 50 minutes.

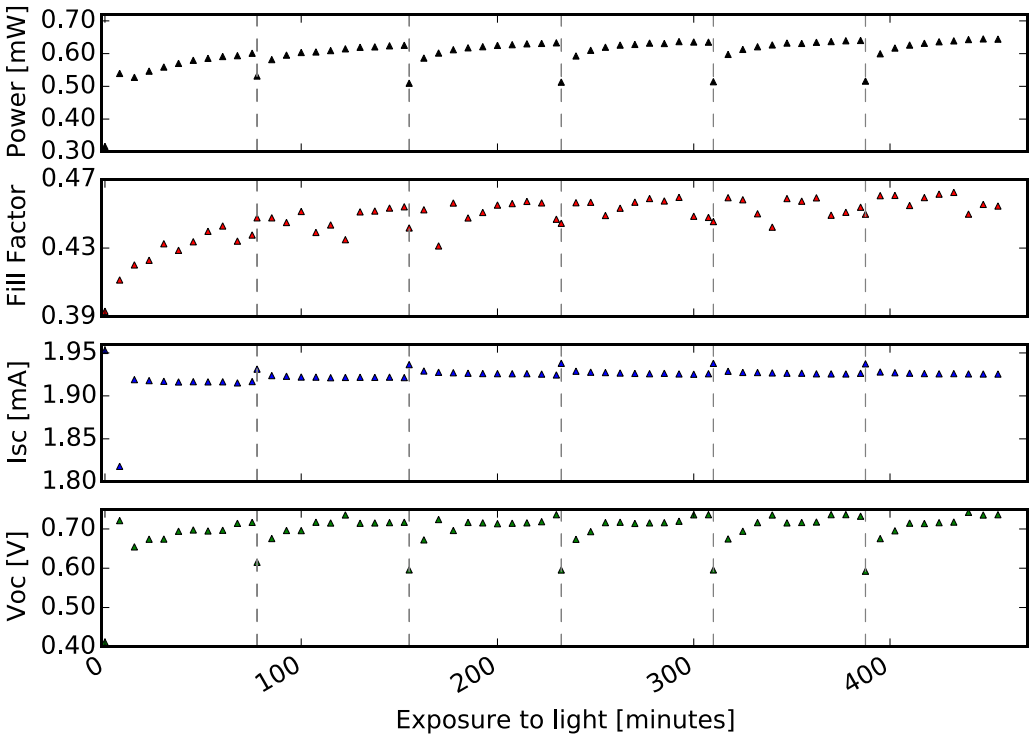

Figure 29: OP 10 I-V forward scan, influence of light soak on different parameters of the cell, the dashed lines indicate a relaxation time in the dark of 1 hour, points on the dashed line were taken directly after the time in the dark

The dotted vertical lines indicate a relaxation time in the dark under short circuit conditions. The measurement on the line is taken without any light soak after this time in the dark. The cell does not return to its initial state after 1 hour in the dark but shows a much higher value for power and V_{oc} in comparison to the initial one (0.5 mW or 0.6 V compared to 0.3 mW and 0.4 V). In addition the cell returns faster to a high power state compared to the first light soak (first light soak 0.6 mW in 70 minutes, second light soak after the first dark period 0.6 mW in 20 minutes). The power rises even further, more time given. That indicates a memory effect for the cell, reaching back further than 1 hour. The cell remembers being light soaked.

To understand how long that memory effect reaches back, the cell was given different amounts of time in the dark before the same set of experiments (with less repetitions) has been carried out.

Leaving the cell in the dark for three hours results in a V_{oc} of 0.53 V and a power of 0.45 mW (Figure 30). These values is much higher than the initial values of the first light soak (0.3 mW and 0.4 V) indicating that the memory has so far not been successfully cleared.

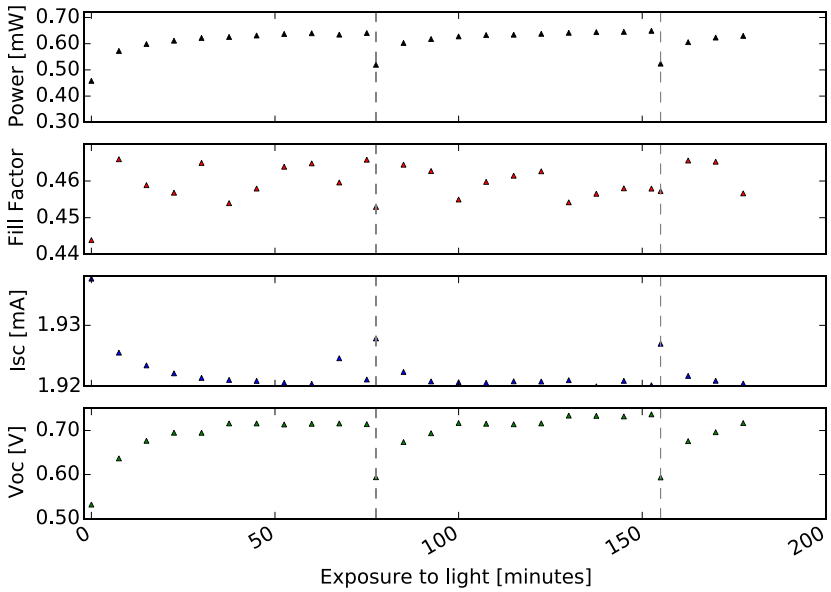

Figure 30: OP 10, 3 hours relaxation in the dark between last light soak and this experiment's start, I-V forward scan, influence of light soak on different parameters of the cell, the dashed lines indicate a relaxation time in the dark of 1 hour, points on the dashed line were taken directly after the time in the dark

Leaving the cell for six hours in the dark, the cell does not reach its initial state as it can be seen in Figure 31 but still shows high values (0.4 mW and 0.5 V).

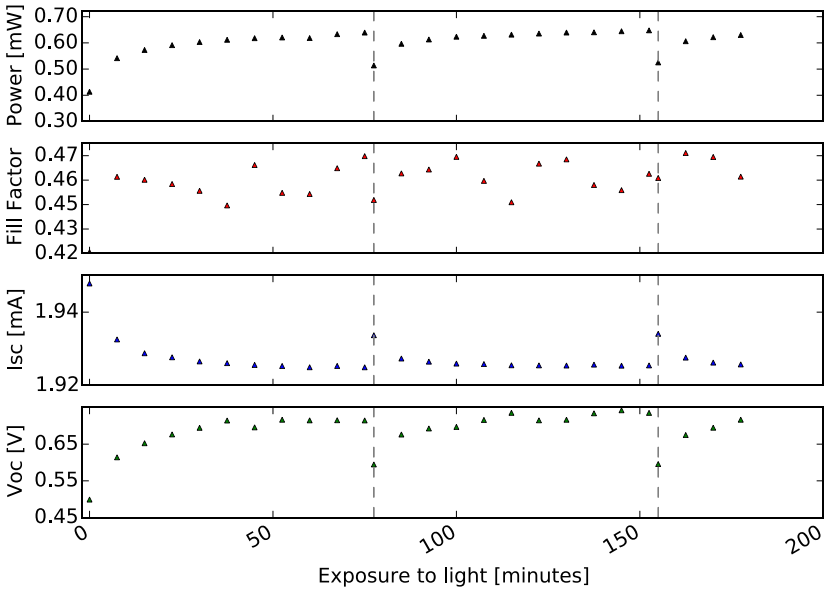

Figure 31: OP 10, 6 hours relaxation in the dark between last light soak and this experiment's start, I-V forward scan, influence of light soak on different parameters of the cell, the dashed lines indicate a relaxation time in the dark of 1 hour, points on the dashed line were taken directly after the time in the dark

12 hours in the dark (Figure 32) result in a power of 0.38 mW and a Voc of 0.45 V. After 12 hours in the dark the cell still shows higher values compared to the initial light soak and therefore shows a memory effect lasting longer this time period.

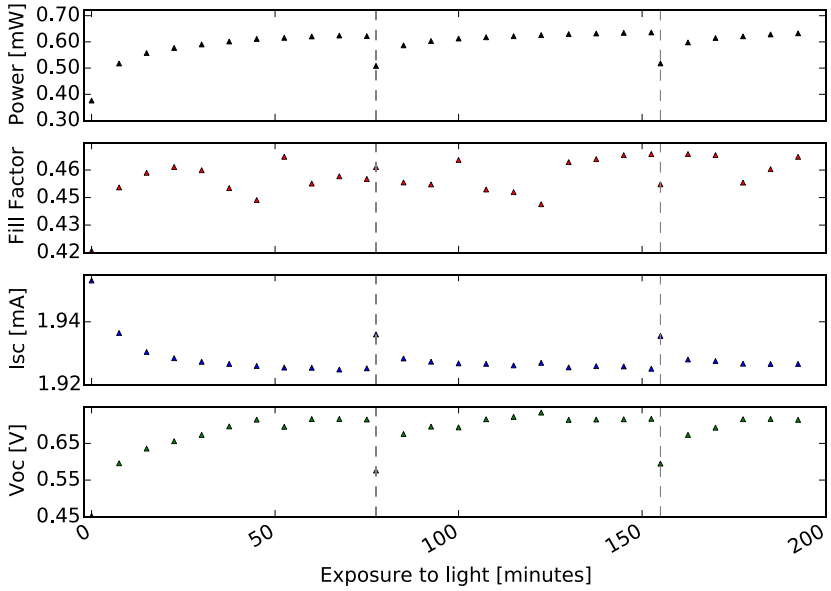

Figure 32: OP 10, 12 hours relaxation in the dark between last light soak and this experiment's start, I-V forward scan, influence of light soak on different parameters of the cell, the dashed lines indicate a relaxation time in the dark of 1 hour, points on the dashed line were taken directly after the time in the dark

In Figure 33 the initially measured power, I_{sc} and V_{oc} values at time = 0 for each run (3, 6 and 12 hours in the dark) are plotted with an indication of the original initial values (from Figure 29). A linear fit to that data suggests that the memory effect reaches back up to 16 hours. Unfortunately time was too limited to conduct an additional experiment to further quantify the memory effect.

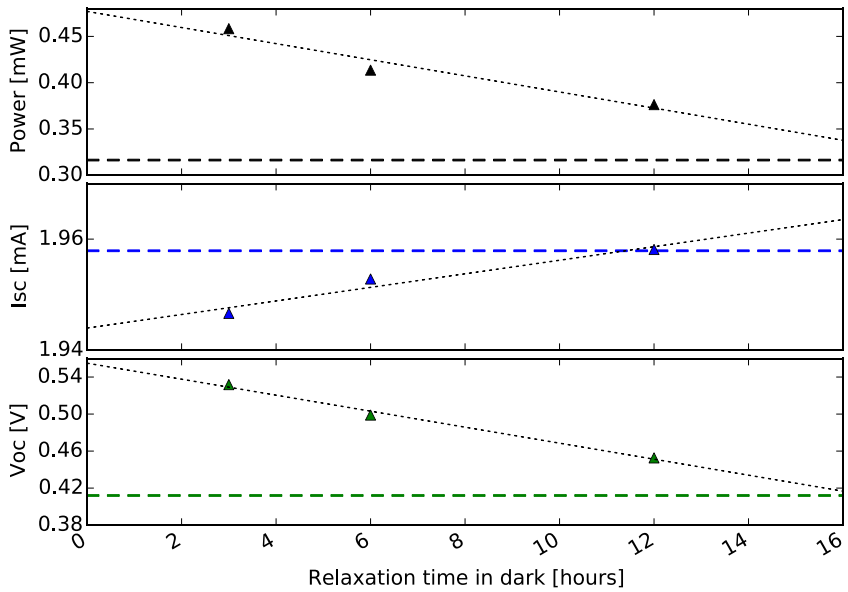

Figure 33: Change of initially measured values (with dotted line as trendline) after relaxation times in the dark compared to the original power, short circuit current and open circuit voltage values (dashed line)

4.7 MEMORY EFFECT IN THE W CELL AND CURRENT RETARDATION

Waiting time experiment

The aim of the waiting time experiment is the determination of a relaxation time in the dark for the process that retards charge carriers during light soaks and the reestablishment of the default cell properties.

The cell is illuminated for a defined period, then given the chance to relax in the dark for different times and illuminated again for the same period. A set of experiments sums up to about 2 hours of illumination and testing of the cell distributed over a total time of six hours, whereas the cell is left shortened in the dark otherwise. Different light levels are used to illuminate the cell. This set is then repeated several times with six hour periods shortened in the dark in between two sets. The transient behaviour is measured at short circuit mode, the applied voltage is 0 V and the cell temperature 25 °C.

Looking at the transient current response of the W cell to a light soak, a retardation of the current starting roughly five seconds after the light soak and resulting in a dip with a peak at 25 seconds can be observed (Figure 35). That dip is most distinct if the cell has not been illuminated or subject to measurements for several days. Giving the cell no relaxation time at all between light soaks (in fact some few ms that it takes the software to start the next measurement procedure) the dip cannot be observed at all and the current reaches a stable value in few seconds. Leaving the cell in dark under short circuit condition for 45 up to 80 minutes and light soaking it afterwards, results in a transient signal that changes its magnitude dramatically (13 %) and takes 600 or even more seconds to stabilize.

The shape of this signal resembles the initial dip that can be observed if the cell has not been tested for days. Interestingly it seems that a relaxation time for more than 45 minutes reduces the dip. But it is likely that another effect is influencing that measurement.

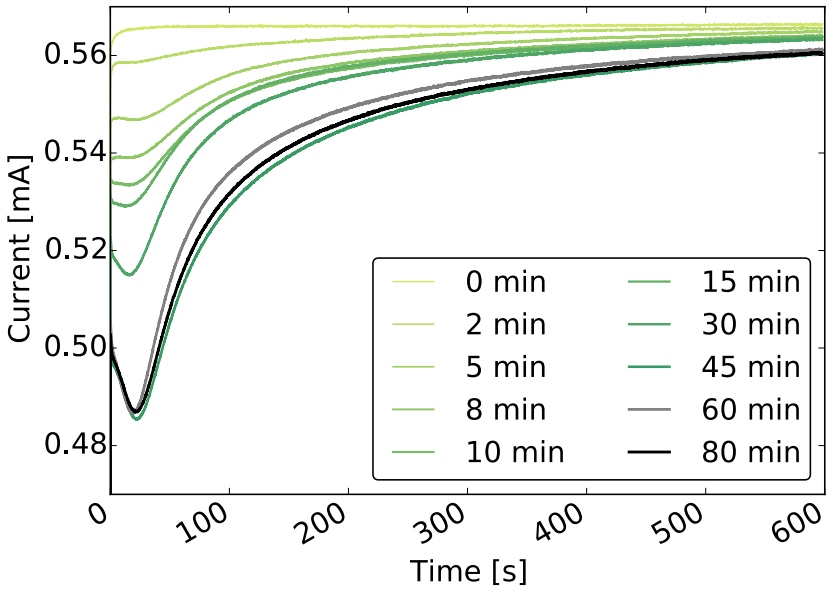

Figure 35: W cell, Current retarding dip during light soak occurring with different strength depending on the relaxation (given in minutes) time in between experiments (shortened and in the dark) cell kept at 25°C

The same experiment has been carried out for different light levels. All different light levels (0.4, 0.8 and 2 suns) and repetitions show the same behaviour. The longer the relaxation time in the dark, the stronger the dip's influence (Figure 34). But it remains only a trend since the data seems not to be reproducible even though the experiment was carried out under nitrogen atmosphere, very stable temperature and light conditions and further on in a randomized order. Excluding the light and temperature effects, changes over time within the cell remain as an explanation.

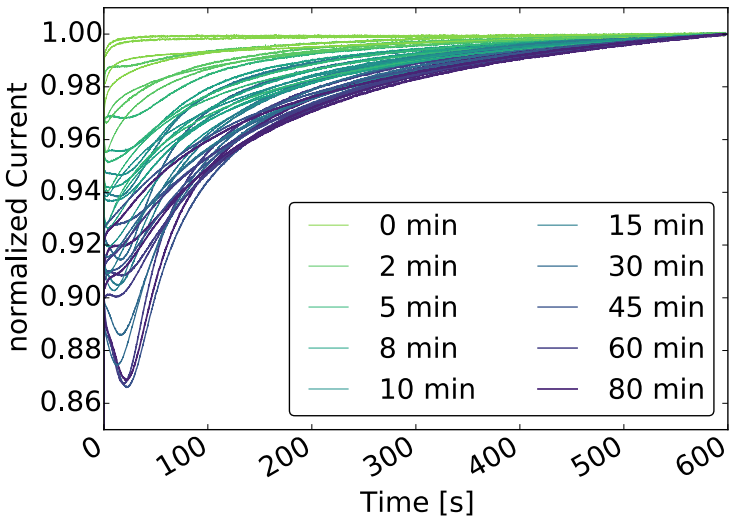

Figure 34: W cell, dip for different relaxation times, 4 repetitions of the experiment, at 25°C

Looking at all the transients (including different light levels) arranged by the time they were carried out, a general decrease of the dip with an increasing number of experiments can be stated. This effect can be seen in Figure 36 where early experiments were marked in dark colour

and later ones in lighter colours. Since all graphs refer to different waiting times, there are also dark graphs with a small up to no dip. But no a single light coloured graph shows the dip.

All of the late experiments are less strong influenced by the current retardation. The cell appears to have a memory effect reaching back some hours.

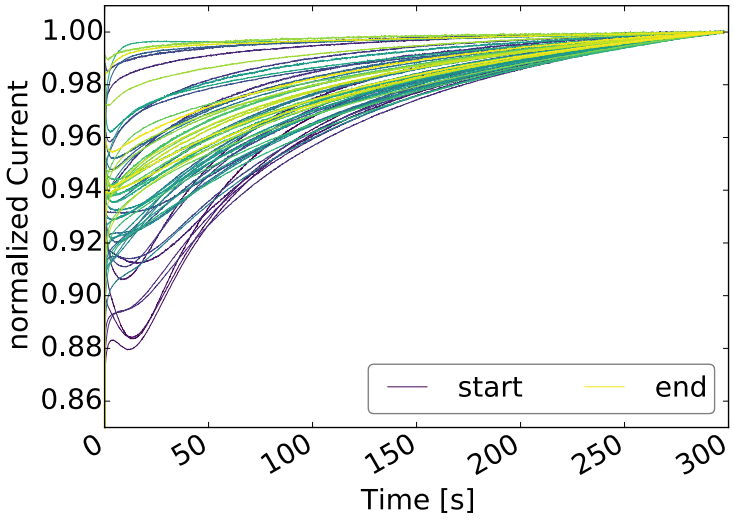

Figure 36: W cell, light soak transient current responses in the order they were taken, different light levels but all at 25°C

To get a clearer picture four transient responses with the same measurement setup were recorded. After an initial light soak a set of experiments was conducted and the cell left shortened in the dark for six hours to return to its initial state. This procedure was repeated four times and the four "initial" light soaks are shown in Figure 37.

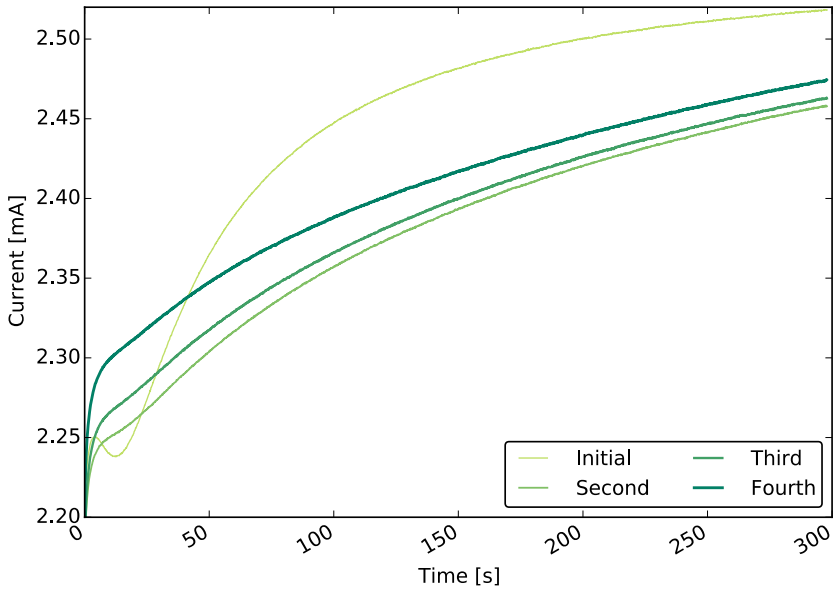

Figure 37: Dip and non-reproducibility of transient current response of W cell to light soak even after six hours relaxation between each measurement

Neither show the second, third or fourth initial light soak the same behaviour as the first. Only the first light soak displays the dip (prior to that light soak the cell has not been illuminated or tested for a longer period of time). These results indicate the existence of a memory effect that reaches back more than six hours. In fact reproducible measurements were possible after leaving the W cell two days un-probed in the dark. A one day lasting waiting time (about 24 hours) did not result in a full clearance.

Most likely the unexpected less distinct feature in the transient response of the 60 and 80 minute relaxation time compared to the 45 minute response can be accounted to that memory effect.

The reason for the charge retardation seem to appear and disappear within not more than 300 seconds in the light but takes 45 minutes in the dark to return to its initial state. That indicates a much higher movement speed for these particles in the light than in the dark.

Perovskite cells are known to display polarization effects and ionic movement (Chapter 2) and the calculation of the activation energy suggests the possibility of ionic participation in the current generation process. The stated time frames are too high for only electrons. An explanation for the difference in the movement speed under illumination and in the dark could be ions, overcoming the activation energy level due to the additional energy provided by the light. That suggests mostly ionic movement within the cell, as a reason for the retardation of the current output.

In order to quantify the retardation, the number of retarded charges (and hence possible charge traps or ions) can be calculated as follows:

$$I = \frac{dQ}{dt} \quad \rightarrow \quad Q = \int I \, dt$$

With n_{charge} as the amount of charges

$$n_{charge} = \frac{Q}{elementary\ charge} \quad \rightarrow \quad n_{charge} = \frac{\int I \, dt}{elementary\ charge}$$

The number of retarded charges n_r for each waiting time t is then calculated via the subtraction of the charges at that particular waiting time ($n_{charge(t)}$) from the charges at the waiting time 0 minutes ($n_{charge(0)}$) .

$$n_{r(t)} = n_{charge(0)} - n_{charge(t)}$$

A visualization of the calculations is given in Figure 38. The areas formed by the initial graph of zero minutes relaxation time and all other graphs are calculated (in this example 45 minutes indicated in olive green in Figure 38 top right). The $Q_{0\ minutes}$ area, indicated in olive green in Figure 38 top left, is regarded as the steady state reference value. As the cell is not given any time to return to its initial state this area is the largest of all.

The calculated areas of the retarded current are subtracted from this reference area. The resulting areas are a measure for the retarded current for each specific relaxation time.

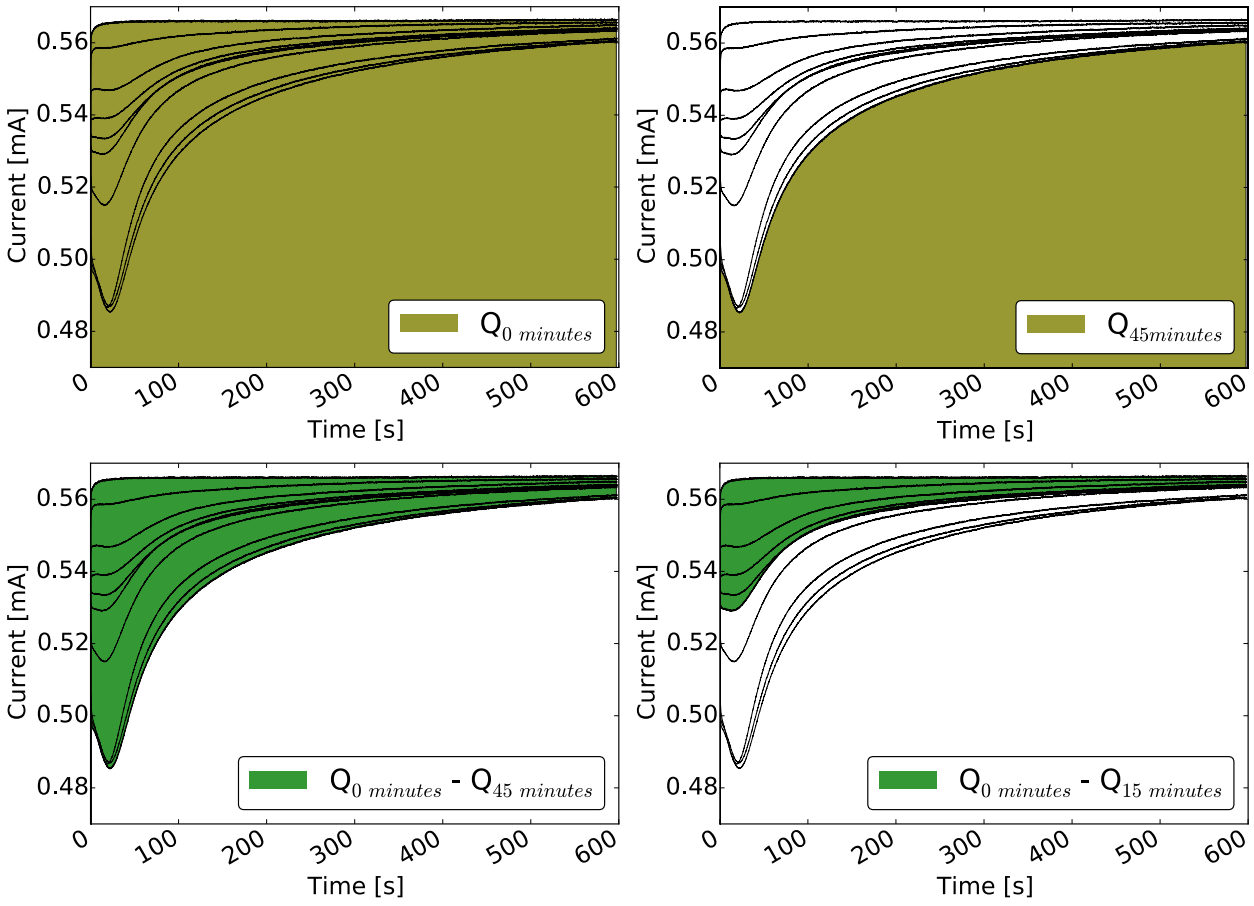

Figure 38: Graphical illustration of the charge calculation

Approximating the number of retarded charges by applying the Riemann sum, a retardation of roughly 3.8 % of the overall current can be observed as seen in Figure 39 and a single exponential curve can be fit to the data of relaxation process. The amount of retarded charges is normalized to the highest occurring value ($n_{r(45)}$) and also given as a percentage of the non retarded charges ($n_{charge(0)}$).

The values of the 60 and 80 minutes relaxation time are lower than the 45 minute value. That unexpected behaviour might be caused by the memory effect that might have adulterated the whole dataset. Therefore these findings in particular are used to illustrate trends rather than displaying absolute values.

That exponential convergence process could be explained by ions moving back to their original state.

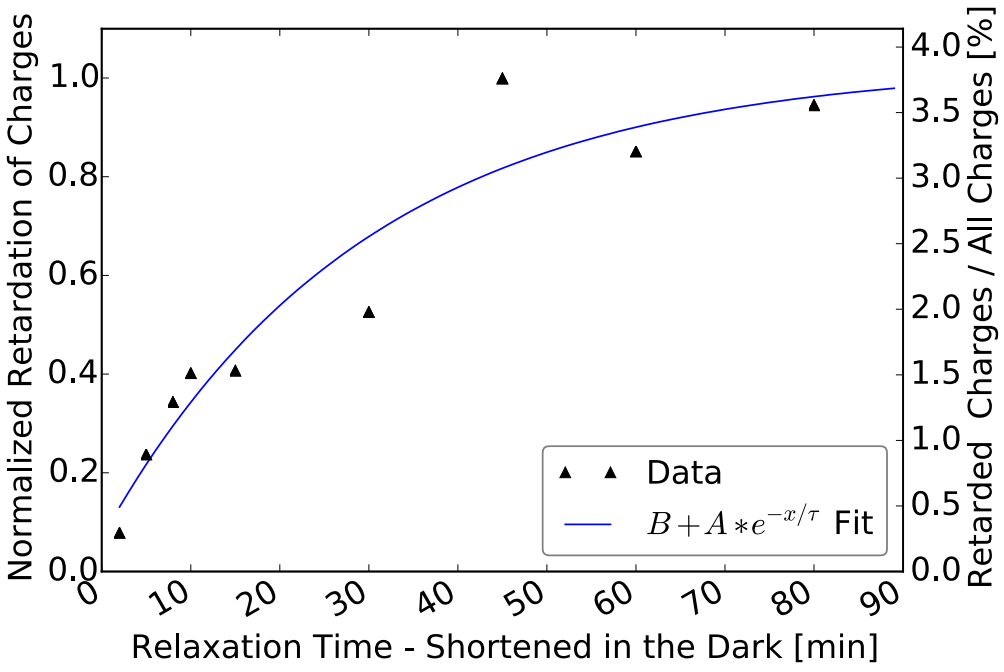

Figure 39: Retarded charges normalized to the maximum retarded charges at 45 minutes and as a percentage of all charges in dependency of relaxation time in the dark under short circuit condition

As ions are suspected to cause the retardation, I^- is the most likely candidate, with the lowest activation energy (0.58 eV [26]) of all three ions, that lies in addition in the range of the calculated activation energy (0.39-0.61 eV).

Having a closer look at the dynamics of the retardation (Figure 40) an increase of the retardation from 0 to about 50 seconds can be observed. That might be attributed to ions overcoming the activation energy empowered by the illumination. After 50 seconds that process might balance out with the process of charge generation so that lattice vacancies become saturated, leading to an exponential decay of the retarded charges afterwards.

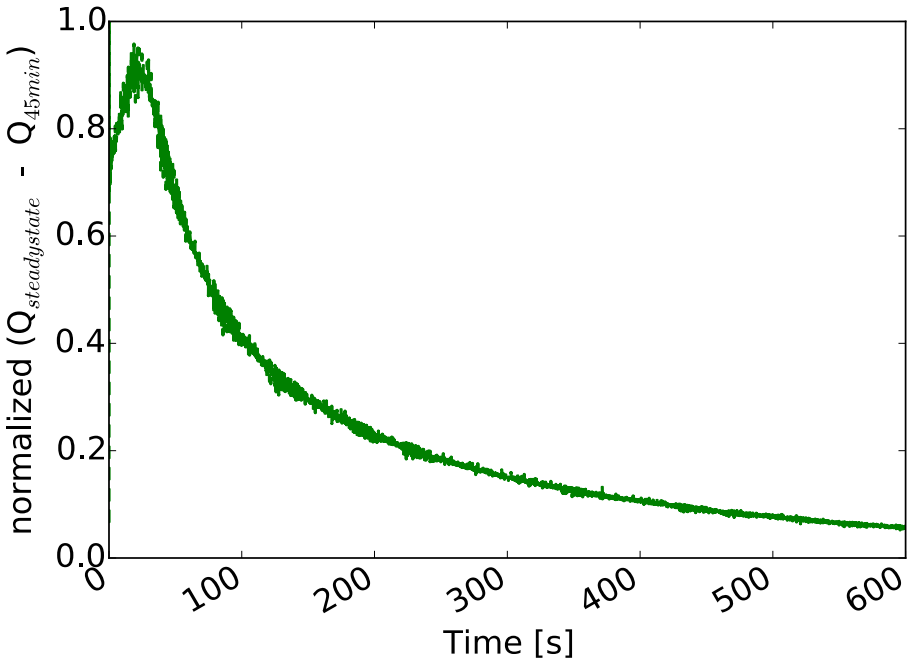

Figure 40: Difference in charges between the 0 min (steady) state compared to the 45 minute waiting time state over time

The retarded charges in absolute values are displayed in Table 5

All Charges [e]	**$2.11607904073 \times 10^{18}$**
Relaxation Time [minutes]	**Approximate Retarded Charges [e]**
2	6.25×10^{15}
5	1.89×10^{16}
8	2.73×10^{16}
10	3.20×10^{16}
15	3.24×10^{16}
30	4.19×10^{16}
45	7.95×10^{16}
60	6.78×10^{16}
80	7.52×10^{16}

Table 5: Approximated amounts of retarded charges

Bias preconditioning experiment

The memory of the cell is fully cleared by waiting time in the dark that is sufficiently long. In the case of the W cell, two days in the dark were enough for the cell to fully recover. These long waiting times result in very time consuming measurements and a conflict with the potentially fast degrading Perovskite material. Therefore the attempt is made to accelerate that process and clear the cell's memory within few minutes.

Designed as a try to negate the memory effect, the aim of this experiment is the determination of the influence of a pre biasing of the cell on the transient current behaviour. For a short time period a bias is applied in the dark then the light is turned on and the transient behaviour is measured, the applied voltage is 0 V. The experiment is carried out with a cell temperature of 25 °C and an illumination of 100%.

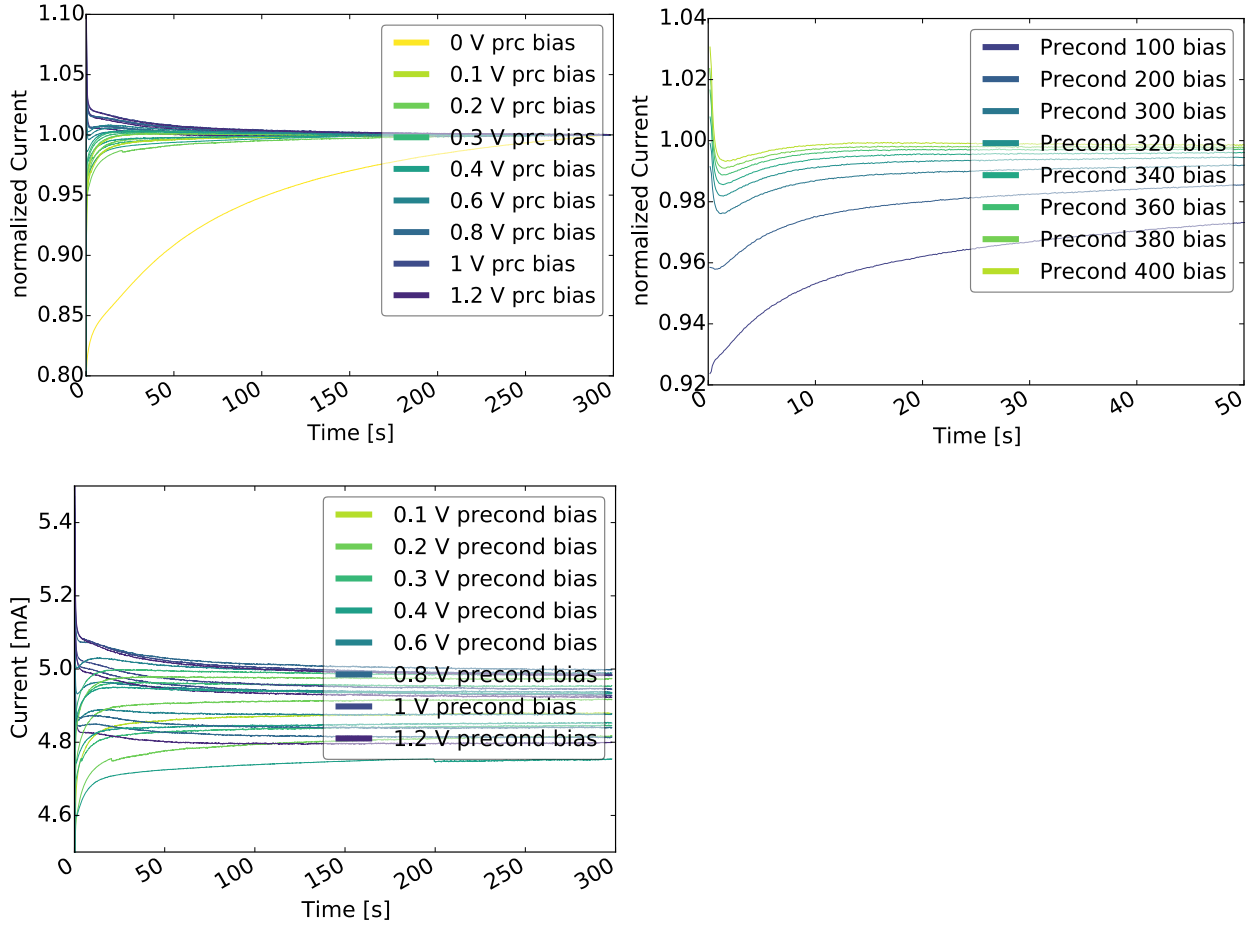

Figure 41: Preconditioning the W cell in the dark at 25 °C with electrical bias from 0 to 1.2 V (several randomized subsequent runs, figure top left) and a more detailed range from 100 to 400 mV bias (single run, figure top right), then light soaking it starting at t = 0. Normalized as well as absolute values (figure bottom left) are shown

As ions are suspected to cause the memory effect, a voltage application strikes as reasonable attempt to force them back into their initial position. That voltage application is carried out in the dark.

The try to reset the memory effect with an electrical biasing of the cell in the dark, prior to the light soak, is partially successful but does not result in a complete reset.

As a starting point the 0 V bias transient behaviour is measured as an initial state. The result displayed in Figure 41 (yellow line top left), looks very similar to the already influenced second, third and fourth measurement in Figure 37. Hence the memory effect is significantly influencing the cell.

The application of a positive bias does change the transient current response of the cell and results in a small dip for an applied voltage of 300 up to 400 mV (detailed view in Figure 41, top right). It starts to appear at 200 mV, is most pronounced at 300 mV and decreases as the voltage is increase up to 400 mV. The feature is nearly as severe as in the totally relaxed state seen in Figure 35. Still, a partial clearance of the memory can be stated as that unique shape is reproduced.

Investigating the magnitude of the current (Figure 41, bottom left), differences of up to 4 % regarding the stabilized current for different runs can be observed. That fact indicates that the memory has not been effectively cleared.

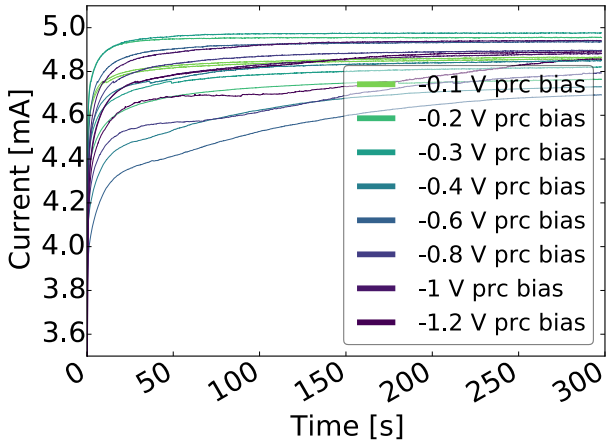

Figure 42: Several runs of light soak of the W cell with prior negative bias (-0.1 to 1.2 V) preconditioning at 25°C

Applying a negative bias as a preconditioning treatment does not show the slightest indication of a memory clearance as shown in Figure 42. Repeated measurements of the same voltage pre-biasing differ not only in the magnitude of the stabilized current but further on do not show the feature.

A partial clearance of the memory effect seems possible for certain voltages but a complete erasure has not been achieved using the preconditioning in the dark method.

As shown earlier, the dip itself vanishes after hundred or some hundreds of seconds under illumination whereas the cell takes at least 45 minutes in the dark to recover. Derived from that a voltage pre-biasing of the cell in the light appears to be a promising approach.

First measurements under non-comparable conditions (uncertain cell history, non-controlled temperature, non-comparable irradiance level) seemed promising but unfortunately the W cell got destructed due to overheating of the dry cabinet before trustable data could be gathered.

The waiting time experiments have been carried out for the OP 10 cell but no retardation of the current can be observed. All of the transient measurement results in Figure 43 overlay each other. OP 10 shows an extraordinary reproducibility of transient measurements.

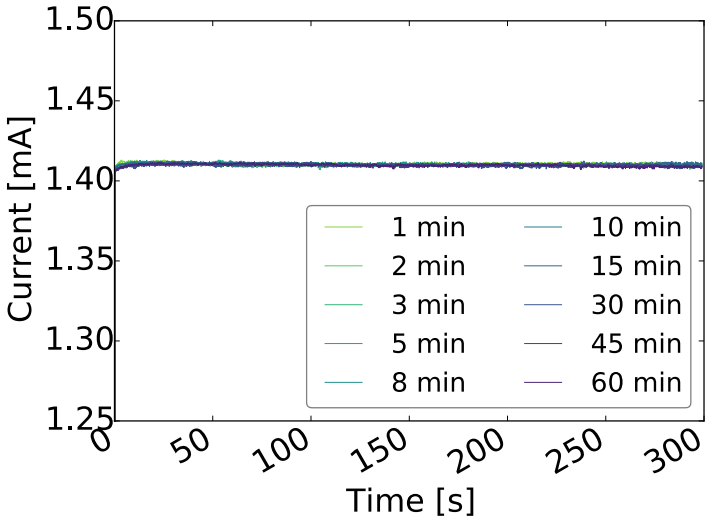

Figure 43: Light soak OP 10 with different waiting times in the dark

That fits the results of the activation energy calculation well, which assume a minor role of ionic movement in OP 10 cell's current distribution.

Verification of the trustworthiness of the partial memory clearance

The partial clearance of the memory effect might be real but could also be confused with a feature caused by the voltage pre-biasing itself. In order to rule such an effect out, the same voltage pre-biasing is applied to OP 10 which under normal conditions shows no dip at all.

Therefore confidence in the partial clearance of the memory effect can only be gained, if no dip is seen in the result of the identical experiment carried out for OP 10.

The verification, that the reproduction of the dip (Figure 41, top right) is specific to the W cell, can be seen in Figure 44.

Pre-conditioning with different voltages affects the transient current behaviour similarly to the results presented for the W cell. The current rises and the time it takes to stabilize (settling time), reduces from negative and to small positive biases and is almost zero for 400 mV. As the bias is further increased, the settling time increases, but now the current decays.

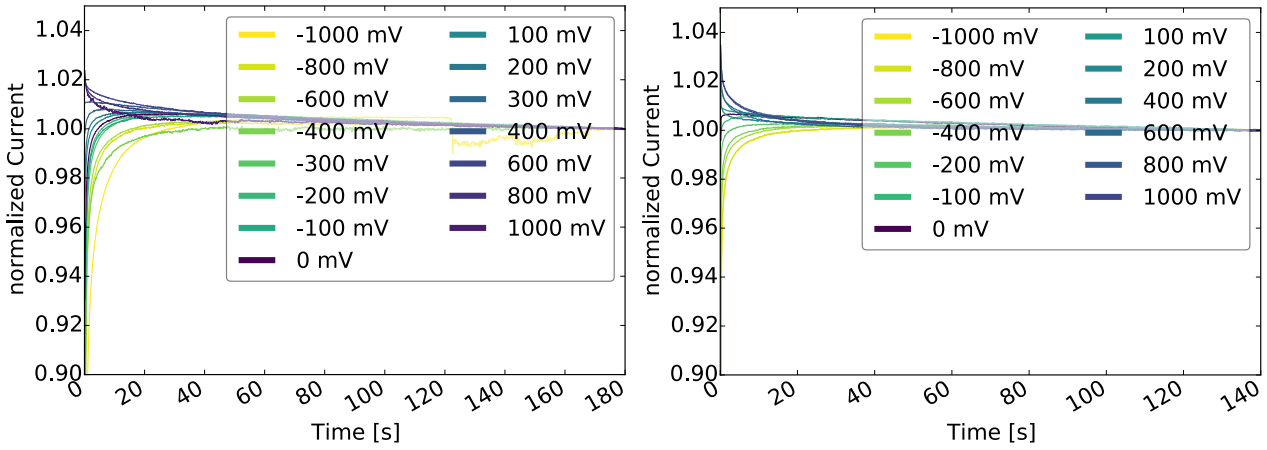

Figure 44: Prebiasing OP 10 with different voltages, then light soak. Preconditioning in the dark on the left and under illumination on the right

But there is an important difference. In a certain voltage range (200-400 mV) the W cell does show the dip. That dip cannot be found for OP 10 at any pre-biasing voltage.

It can be confidently assumed that the partial clearance of W cell's memory was successfully performed.

5 CONCLUSION

A concept to estimate appropriate dwell time was proposed and tested for dye cells. It does work in that case and can most probably be applied to perovskite cells as well. Trouble regarding the application of that method to Perovskite cells did occur, in form of measurement equipment that is not able to record high resolution time resolved current behaviour in the time regime of minutes and a memory effect that this study found to be present for the investigated Perovskite cells. This effect makes reproducible transient measurements hard to achieve and very time consuming. With the knowledge of that effect, a reliable method of clearing the cell's memory and measurement equipment suited for that specific time frame, the dwell time estimation method might be successfully applied to Perovskite cells.

The influence of the irradiance level, temperature and time (light soak or relaxation in the dark) on the Perovskite cells was studied.

Regarding the effect of temperature, the fill factor and V_{oc} were found to be strongly temperature related, rising by up to 100 % (V_{oc}) and 20 % (FF rises and diminishes again) for the OP 10 and OP 7 cell over a temperature range of 40 K. Opposing to that only minor changes in I_{sc} were observed (drop by no more than 3.5 %). Both OP cells show positive temperature dependency for Voc and FF and negative temperature dependency for I_{sc}. Looking at the W cell a negative temperature dependency for V_{oc} with a drop of 25 % and a positive temperature dependency for I_{sc} (25% rise) and FF (80 % rise) is observed. The fact that two cells of the same cell type show different temperature dependencies (positive in one case and negative in the other case) has to be stressed. Since the exact components of the OP cells remain unknown it is likely that they differ from the ones in the W cell. Generalized it can be concluded that the inverted structure cells are heavily affected by temperature, yet the effect has to be quantitatively determined for each cell type. Maintaining a stable cell temperature during measurement is important.

The irradiance level has a direct influence on OP 10's short circuit current as well as maximum power point. A linear dependency of both parameters on the irradiance level was found. The higher the irradiance level, the higher the short circuit current and the power.

The problem of a poor reproducibility of transient measurement results for Perovskite cells (especially cell W-7-6.1) has been noticed and investigated.

Both, the OP 10 and W cell, suffer from memory effects reaching back multiple hours. Even though it is expressed by the cells in different ways that phenomena negatively affects the reproducibility of transient measurements. Regarding the W cell, the current's transient

behaviour changes the longer the cell is exhibited to light and probed but returns to its initial behaviour if once the memory is cleared. Looking at the OP 10 cell I-V curve measurements are observed to benefit from a light soaking memory effect as the cell remembers that it has been light soaked and returns to high V_{oc} and power values faster compared to the initial light soak.

The memory effect is responsible for troublesome measurements of the electrical properties of the cell even though other effects might contribute additionally. Clearing the memory effect is possible by leaving the cell un-probed in the dark for one day in case of OP 10 or two days in case of the W cell. Attempts to entirely clear the memory within few minutes via applying a range of voltage biases without illumination, result in a partial memory clearance. It was found in this study that the charge retarding particles move faster in the light than in the dark. Therefore the voltage biasing as pre-treatment experiment carried out under illumination is proposed as a promising method to entirely clear the memory.

6 OUTLOOK

Not knowing about the memory effect, reproducible transient measurements are hardly obtained. With the investigation of the memory effect in this study, in addition to light and temperature, time is identified as an important physical parameter influencing the cell's performance. This finding enables future research to take that effect into account (during planning of measurements) and enable further work on the memory effect itself.

For future research work it is suggested to investigate the applicability of the dwell time estimation method on perovskite cells, with measurement equipment that supports the required time regime (high resolution in minute range) and under consideration of the memory effect. The investigation of more cells of different structure and their activation energy levels in correlation with the presumably ionic current retardation might be of interest.

A method of fully clearing the memory of the cell would massively reduce the time amount needed to conduct experiments in a reproducible way. Therefore the investigation of the accelerated memory clearance is recommended as a starting point for future research.

The dynamics of charge retardation as seen in Figure 40 might bear information about lattice defects and ionic movement as well as polarization effects within the Perovskite material. It might be possible to establish a categorisation of the cell's properties or bahaviour by comparing different cell's graph shape of charge retardation dynamics. Investigations heading in that direction might be worthwhile.

7 REFERENCES

[1] H. J. Snaith, A. Abate, J. M. Ball, G. E. Eperon, T. Leijtens, N. K. Noel, S. D. Stranks, J. T. Wang, K. Wojciechowski, and W. Zhang, "Anomalous Hysteresis in Perovskite Solar Cells," *J. Phys. Chem. Lett.*, vol. 5, pp. 1511–1515, 2014.

[2] W. Tress, N. Marinova, T. Moehl, S. M. Zakeeruddin, M. K. Nazeeruddin, and M. Grätzel, "Understanding the rate-dependent J–V hysteresis, slow time component, and aging in CH3NH3PbI3 perovskite solar cells: the role of a compensated electric field," *Energy Environ. Sci.*, vol. 8, pp. 995–1004, 2015.

[3] E. L. Unger, E. T. Hoke, C. D. Bailie, W. H. Nguyen, A. R. Bowring, T. Heumuller, M. G. Christoforo, and M. D. McGehee, "Hysteresis and transient behavior in current-voltage measurements of hybrid-perovskite absorber solar cells," *Energy Environ. Sci.*, pp. 3690–3698, 2014.

[4] R. B. Dunbar, T. W. Jones, K. F. Anderson, G. J. Wilson, C. J. Fell, *An Investigation of Perovskite Solar Cell Degradation and I-V Hysteresis for Improved Accuracy of Efficiency Measurements at Standard Test Conditions*, vol. 1. 2015.

[5] M. a. Green, A. Ho-Baillie, and H. J. Snaith, "The emergence of perovskite solar cells," *Nat. Photonics*, vol. 8, no. 7, pp. 506–514, 2014.

[6] Y. Wang, Y. Zhang, peihong zhang, and W. Zhang, "High intrinsic carrier mobility and photon absorption in perovskite CH3NH3PbI3," *Phys. Chem. Chem. Phys.*, Mar. 2015.

[7] J. Ma and L. Wang, "Nanoscale Charge Localization Induced by Random Orientations of Organic Molecules in Hybrid Perovskite CH 3 NH 3 PbI 3," *Nano Lett.*, vol. 15, p. 248, 2015.

[8] J. Qing, H. T. Chandran, H. T. Xue, Z. Q. Guan, T. L. Liu, S. W. Tsang, M. F. Lo, and C. S. Lee, "Simple fabrication of perovskite solar cells using lead acetate as lead source at low temperature," *Org. Electron. physics, Mater. Appl.*, vol. 27, pp. 12–17, 2015.

[9] J. A. Christians, J. S. Manser, and P. V Kamat, "The Multifaceted Excited State of CH 3 NH 3 PbI 3 . Charge Separation, Recombination, and Trapping," *J. Phys. Chem. Lett.*, vol. 6, no. 11, p. 150514080751001, 2015.

[10] M. B. Johnston and L. M. Herz, "Hybrid Perovskites for Photovoltaics: Charge-Carrier Recombination, Diffusion, and Radiative Efficiencies," *Acc. Chem. Res.*, p. acs.accounts.5b00411, 2015.

[11] E. J. Juarez-Perez, R. S. Sanchez, L. Badia, G. Garcia-Belmonte, Y. S. Kang, I. Mora-Sero, and J. Bisquert, "Photoinduced giant dielectric constant in lead halide perovskite solar cells," *J. Phys. Chem. Lett.*, vol. 5, no. 13, pp. 2390–2394, 2014.

[12] G. Xing, N. Mathews, S. Sun, S. S. Lim, Y. M. Lam, M. Gratzel, S. Mhaisalkar, and T. C. Sum, "Long-Range Balanced Electron- and Hole-Transport Lengths in Organic-Inorganic CH3NH3PbI3," *Science (80-.).*, vol. 342, no. 6156, pp. 344–347, Oct. 2013.

[13] K. Tanaka, T. Takahashi, T. Ban, T. Kondo, K. Uchida, and N. Miura, "Comparative study on the excitons in lead-halide-based perovskite-type crystals CH3NH3PbBr3 CH3NH3PbI3," *Solid State Commun.*, vol. 127, no. 9–10, pp. 619–623, Sep. 2003.

[14] F. J. Ramos, D. Cortés, A. Aguirre, F. J. Castaño, and S. Ahmad, "Fabrication and encapsulation of perovskites sensitized solid state solar cells," pp. 2–4, 2014.

[15] Y.-C. Hsiao, T. Wu, M. Li, Q. Liu, W. Qin, and B. Hu, "Fundamental Physics behind High-Efficiency Organo-Metal Halide Perovskite Solar Cells," *J. Mater. Chem. A*, May 2015.

[16] S. D. Stranks, G. E. Eperon, G. Grancini, C. Menelaou, M. J. P. Alcocer, T. Leijtens, L. M. Herz, a. Petrozza, and H. J. Snaith, "Electron-Hole Diffusion Lengths Exceeding 1 Micrometer in an Organometal Trihalide Perovskite Absorber," *Science (80-.).*, vol. 342, no. 6156, pp. 341–344, Oct. 2013.

[17] S. Kumari, S. K. Jain, B. K. Das, and G. C. Jain, "On the effective minority carrier diffusion length of polycrystalline silicon solar cells," *Sol. Cells Their Sci. Technol. Appl. Econ.*, vol. 9, no. 3, pp. 209–214, 1983.

[18] M. Hirasawa, T. Ishihara, T. Goto, K. Uchida, and N. Miura, "Magnetoabsorption of the lowest exciton in perovskite-type compound (CH3NH3)PbI3," vol. 201, pp. 427–430, 1994.

[19] N. C. Giebink, G. P. Wiederrecht, M. R. Wasielewski, and S. R. Forrest, "Thermodynamic efficiency limit of excitonic solar cells," *Phys. Rev. B - Condens. Matter Mater. Phys.*, vol. 83, no. 19, pp. 1–6, 2011.

[20] K. T. Butler, J. M. Frost, and A. Walsh, "Band alignment of the hybrid halide perovskites CH3NH3PbCl3 , CH3NH3PbBr3

and," *Mater. Horizons*, vol. 2, pp. 228–231, 2015.

[21] D. Shi, V. Adinolfi, R. Comin, M. Yuan, E. Alarousu, A. Buin, Y. Chen, S. Hoogland, A. Rothenberger, K. Katsiev, Y. Losovyj, X. Zhang, P. A. Dowben, O. F. Mohammed, E. H. Sargent, and O. M. Bakr, "Low trap-state density and long carrier diffusion in organolead trihalide perovskite single crystals."

[22] G. E. Eperon, V. M. Burlakov, P. Docampo, A. Goriely, and H. J. Snaith, "Morphological Control for High Performance, Solution-Processed Planar Heterojunction Perovskite Solar Cells," *Adv. Funct. Mater.*, Sep. 2013.

[23] C. Quarti, E. Mosconi, J. M. Ball, V. D'Innocenzo, C. Tao, S. Pathak, H. J. Snaith, A. Petrozza, and F. De Angelis, "Structural and optical properties of methylammonium lead iodide across the tetragonal to cubic phase transition: implications for perovskite solar cells," *Energy Environ. Sci.*, 2015.

[24] J. M. Frost, K. T. Butler, F. Brivio, C. H. Hendon, M. Van Schilfgaarde, and A. Walsh, "Atomistic origins of high-performance in hybrid halide perovskite solar cells," *Nano Lett.*, vol. 14, no. 5, pp. 2584–2590, 2014.

[25] J. M. Frost, K. T. Butler, and A. Walsh, "Molecular ferroelectric contributions to anomalous hysteresis in hybrid perovskite solar cells," *Apl Mater.*, vol. 2, no. 8, p. 081506, Aug. 2014.

[26] C. Eames, J. M. Frost, P. R. F. Barnes, B. C. O'Regan, A. Walsh, and M. S. Islam, "Ionic transport in hybrid lead iodide perovskite solar cells," *Nat. Commun.*, vol. 6, no. May, p. 7497, 2015.

[27] S. Meloni, T. Moehl, W. Tress, M. Franckevičius, M. Saliba, Y. H. Lee, P. Gao, M. K. Nazeeruddin, S. M. Zakeeruddin, U. Rothlisberger, and M. Graetzel, "Ionic polarization-induced current–voltage hysteresis in CH3NH3PbX3 perovskite solar cells," *Nat. Commun.*, vol. 7, no. May 2015, p. 10334, 2016.

[28] L. Groenendaal, F. Jonas, D. Freitag, H. Pielartzik, and J. R. Reynolds, "Poly(3,4-ethylenedioxythiophene) and its derivatives: past, present, and future," *Adv. Mater.*, vol. 12, no. 7, pp. 481–494, 2000.

[29] G. Greczynski, T. Kugler, and W. R. Salaneck, "Characterization of the PEDOT-PSS system by means of X-ray and ultraviolet photoelectron spectroscopy," *Thin Solid Films*, vol. 354, no. 1, pp. 129–135, 1999.

[30] C. Waldauf, P. Schilinsky, M. Perisutti, J. Hauch, and C. J. Brabec, "Solution-Processed Organic n-Type Thin-Film Transistors," *Adv. Mater.*, vol. 15, no. 24, pp. 2084–2088, 2003.

[31] Q. Wang, Y. Shao, Q. Dong, Z. Xiao, Y. Yuan, and J. Huang, "Large fill-factor bilayer iodine perovskite solar cells fabricated by a low-temperature solution-process," *Energy Environ. Sci.*, vol. 7, p. 2359, 2014.

[32] J. Liu, Y. Wu, C. Qin, X. Yang, T. Yasuda, A. Islam, K. Zhang, W. Peng, W. Chen, and L. Han, "A dopant-free hole-transporting material for efficient and stable perovskite solar cells," *Energy Environ. Sci.*, vol. 7, pp. 2963–2967, 2014.

[33] H. S. Kim and N.-G. Park, "Parameters Affecting I-V Hysteresis of CH 3 NH 3 PbI 3 Perovskite Solar Cells: Effects of Perovskite Crystal Size and Mesoporous TiO 2 Layer," *J. Phys. Chem. Lett.*, p. 140811175830000, 2014.

[34] J.-H. Im, I.-H. Jang, N. Pellet, M. Grätzel, and N.-G. Park, "Growth of CH3NH3PbI3 cuboids with controlled size for high-efficiency perovskite solar cells," *Nat. Nanotechnol.*, vol. 9, no. 11, pp. 927–932, 2014.

8 SUPPLEMENTARY INFORMATION

Used Chemicals and equipment

Chemicals / Devices	Supplier / Manufacturer	Abbreviation
Lead(II)acetate trihydrate 99,999% pure	Aldrich Chemistry	Pb(Oac)2
Methylammonium Iodide, CH_6IN	DyeSol	MA-I
Silver pellets 99,99% pure	Kurt J Lesker	Ag
N,N-Dimethylformamide anhydrous 99,8% pure	Sigma-Aldrich	DMF
Chlorobenzene anhydrous 99,8% pure	Sigma-Aldrich	
2-Propanol	AnalaR NORMAPUR	Isopropanol
Clevios PVP.AI 4083	Heraeus	PEDOT
PCBM IT-5965	Luminescence Technology Coorperation	PCBM
UV Resin XNR 5516 Z-B1	Nagase Chemtex Coorperation	Resin
Hellmanex III	Hellma	Detergent
Spincoater, WS-650Hz-23NPP/Lite	Laurell Technologies	
Custom made evaporation deposition device	Aangstrom Engineers	
Ultrasonic cleaner, WUC D-22H 1.4 kW	Thermoline Scientific	
Plasma cleaner PDC-002	Harrick Plasma	

Table 6: Chemicals and devices used for cell fabrication

Measurement protocols

In the following descriptions of the exact settings for the different transient measurements can be found.

Waiting time experiment

An initial light soak has been carried out first, then a different waiting time in the dark was applied prior to each light soak. The light soaks have been performed for three different irradiance levels.

All of these measurements have been carried out twice and the whole amount of measurements was split into 4 batches with 6 hours of relaxation time, shortened in the dark to avoid memory effects.

All light soaks and waiting times were performed in a randomized order at 298K.

Waiting times Z in minutes = [0, 2, 5, 8, 10, 15, 30, 45, 60, 80]

Initial (=light soak 50%)	Time step [s]	60
Time [s]	**Voltage [V]**	**Light level [%]**
Time step × 0	0	50
Time step × 10	0	0

Light soak 50%	Time step [s]	60
Time [s]	**Voltage [V]**	**Light level [%]**
Time step × 0	0	50
Time step × 10	0	0

Light soak 20%	Time step [s]	60
Time [s]	**Voltage [V]**	**Light level [%]**
Time step × 0	0	20
Time step × 10	0	0

Light soak 10%	Time step [s]	60
Time [s]	**Voltage [V]**	**Light level [%]**
Time step × 0	0	10
Time step × 10	0	0

Waiting time Z minutes	Time step [s]	60
Time [s]	**Voltage [V]**	**Light level [%]**
Time step × 0	0	0
Time step × Z	0	0

Measurement protocol
Initial
Waiting time Z minutes
Light soak 50 %
Waiting time E minutes
Light soak 20 %
Waiting time P minutes
Light soak 50 %
Waiting time O minutes
Light soak 10 %
…

Bias preconditioning in dark experiment for W cell

Several random measurements have been undergone to occupy the memory of the cell

All biasing has been performed in a randomized order at 298K.

Pre bias Z in Volt = [-1.2, -1, -0.8, -0.6, -0.4, -0.3, -0.2, -0.1, 0, 0.1, 0.2, 0.3, 0.4, 0.6, 0.8, 1, 1.2]

Pre Bias Z	Time step [s]	60
Time [s]	**Voltage [V]**	**Light level [%]**
Time step × -1	Z	0
Time step × 0	0	100
Time step × 5	0	0

Measurement protocol
Dummy =Pre Bias 0
Pre Bias 1.2
Pre Bias -0.8
Pre Bias -0.1
Pre Bias 0.4
…

Bias preconditioning in dark experiment for OP 10 cell

All biasing has been performed in a randomized order at 298K.

Pre bias Z in Volt = [-1.2, -1, -0.8, -0.6, -0.4, -0.3, -0.2, -0.1, 0, 0.1, 0.2, 0.3, 0.4, 0.6, 0.8, 1, 1.2]

Pre Bias Z	**Time step [s]**	60
Time [s]	**Voltage [V]**	**Light level [%]**
Time step × -1	Z	0
Time step × 0	0	25
Time step × 2.33	0	0

Measurement protocol
Dummy =Pre Bias 0
Pre Bias 1.2
Pre Bias -0.8
Pre Bias -0.1
Pre Bias 0.4
…

Voltage steps of different sizes #1 W cell

The voltage step sizes Z in Volt = [0.01, 0.025, 0.05, 0.1]

Voltage Step 0.01	**Time step [s]**	60
Time [s]	**Voltage [V]**	**Light level [%]**
Time step × 0	0	100
Time step × 15	0.01	100
Time step × 20	0	0

Measurement protocol
Voltage Step 0.01
Wait in Dark
Voltage Step 0.025
Wait in Dark
Voltage Step 0.05
Wait in Dark
Voltage Step 0.1

Voltage Step 0.025	**Time step [s]**	60
Time [s]	**Voltage [V]**	**Light level [%]**
Time step × 0	0	100
Time step × 15	0.025	100
Time step × 20	0	0

Voltage Step 0.05	**Time step [s]**	60
Time [s]	**Voltage [V]**	**Light level [%]**
Time step × 0	0	100
Time step × 15	0.05	100
Time step × 20	0	0

Voltage Step 0.1	**Time step [s]**	60
Time [s]	**Voltage [V]**	**Light level [%]**
Time step × 0	0	100
Time step × 15	0.1	100
Time step × 20	0	0

Wait in Dark	**Time step [s]**	60
Time [s]	**Voltage [V]**	**Light level [%]**
Time step × 0	0	0
Time step × 5	0	0

Voltage steps of different sizes #2 OP 10 cell

After each experiment there was a waiting time of 10 ms but instead of setting that up as an experiment, it was set in the Paios settings. All experiments were carried out in a randomized order.

Voltage Step 0.01	Time step [s]	1
Time [s]	**Voltage [V]**	**Light level [%]**
Time step × 0	0	100
Time step × 1	0.01	100
Time step × 2	0	0

Voltage Step 0.025	Time step [s]	1
Time [s]	**Voltage [V]**	**Light level [%]**
Time step × 0	0	100
Time step × 1	0.025	100
Time step × 2	0	0

Voltage Step 0.05	Time step [s]	60
Time [s]	**Voltage [V]**	**Light level [%]**
Time step × 0	0	100
Time step × 1	0.05	100
Time step × 2	0	0

Voltage Step 0.1	Time step [s]	60
Time [s]	**Voltage [V]**	**Light level [%]**
Time step × 0	0	100
Time step × 1	0.1	100
Time step × 2	0	0

Light Soak	Time step [s]	60
Time [s]	**Voltage [V]**	**Light level [%]**
Time step × 0	0	100
Time step × 45	0	0

Measurement protocol
Light Soak
Voltage Step 0.025
Voltage Step 0.1
Voltage Step 0.01
Voltage Step 0.05
…

Stepping through I-V curve #1 (Dye cell and silicon photodiode)

Light Soak	Time step [ms]	1
Time [s]	**Voltage [V]**	**Light level [%]**
-180 × Time step	0	100
Time step × 0	0	100
Time step × 7	0.01	100
Time step × 14	0.02	100
Time step × 21	0.03	100
…	…	…

J-V curve of OP 10 after testing

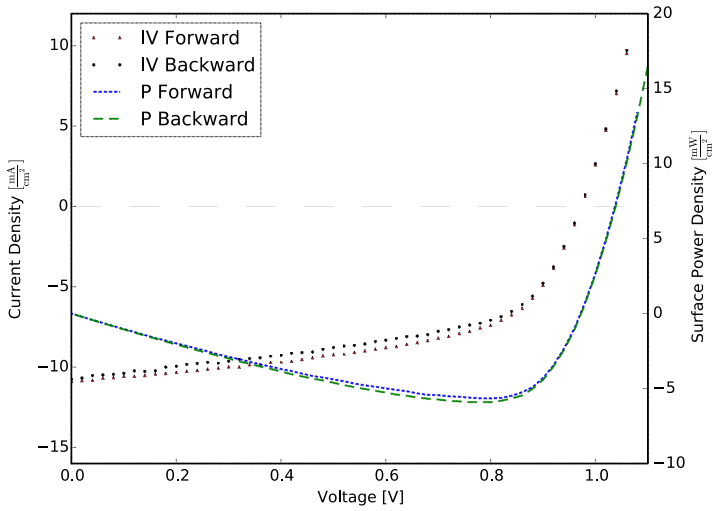

Figure 45: J-V curve of OP 10 cell after 1 month of testing at 25 °C, 1 sun and 45 minutes light soak

J-V curve of OP 7 after testing

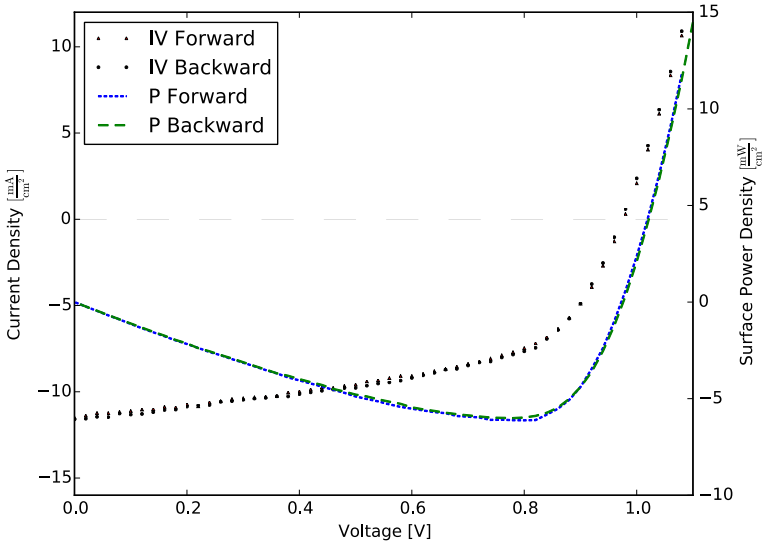

Figure 46: J-V curve of OP 7 after 1 month of testing at 25 °C, 1 sun and 45 minutes light soak

J-V curve of W after testing

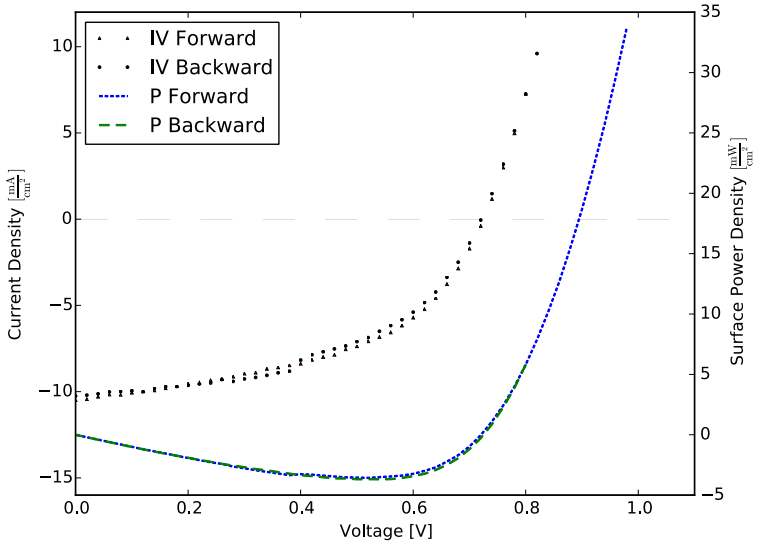

Figure 47: J-V curve of W cell after 2.5 month of testing at 25 °C, 1 sun and 45 minutes light soak